Doctoral Dissertation

Synthesis of thermo- and pH-responsive ampholytic polymeric systems as delivery vehicles

Zhao Dandan

Supervisor: Associate Professor Kazuaki Matsumura

Graduate School of Advanced Science and Technology

Japan Advanced Institute of Science and Technology

[Materials science]

March 2020

Referee-in-chief:

Associate Professor Dr. Kazuaki Matsumura
Japan Advanced Institute of Science and Technology

Referees:

Professor Dr. Noriyoshi Matsumi
Japan Advanced Institute of Science and Technology
Professor Dr. Tatsuo Kaneko
Japan Advanced Institute of Science and Technology
Associate Professor Dr. Eijiro Miyako
Japan Advanced Institute of Science and Technology
Associate Professor Dr. Shin-ichi Yusa
University of Hyogo

Contents

Chapter 1 General introduction

1.1 Intelligent polymer

With the development of science and technology, the functionalization and intelligentization of biological materials has become an important direction for their development. Intelligent polymer materials, also known as stimuli-responsive polymers and environmentally sensitive polymers, are materials that can sense changes in the surrounding environment and cause physical and chemical changes in their conformation, polarity, phase structure, and composition. Due to the unique responsiveness of smart polymers under environmental stimuli, they are widely used in biomedical fields such as cell culture media, controlled-release drug carriers, tissue engineering, molecular diagnostics, and biomimetic materials.[1-7] Depending on the different environmental factors, intelligent polymers can be mainly divided into thermo-responsive polymers, light-responsive polymers, electro-sensitive polymers, magnetic-sensitive polymers, pH-responsive polymers,

enzyme-sensitive polymers, etc. Temperature and pH are the most common stimuli in numerous external environmental stimuli. Therefore, thermo-sensitive and pH-responsive polymers are also the two most widely studied smart polymers.

1.1.1 Thermo-responsive polymer

Thermo-responsive polymer is a type of polymer whose solubility changes with the temperature and have the advantages of easy temperature regulation and no need for additional chemical additives. And the current accepted view of the mechanism of this phase transition behavior is as follows: thermo-responsive polymers generally contain both a hydrophilic group and a hydrophobic group; in the homogeneous phase, thermo-responsive polymers can be dissolved in the solution mainly because the hydrophilic group plays a leading role; when the temperature changes, the interaction between the hydrophilic group and water changes, which causes the balance of the hydrophilic and hydrophobic properties of the polymers to change, and further affects the solubility of the polymers in the solution; and the temperature at which the phase transition occurs is called the phase transition temperature.[8]

1.1.1.1 Type of thermo-responsive polymer

Depending on the phase transition behavior, temperature-responsive polymers can be

classified into two types, the upper critical solution temperature (UCST) type and the lower critical solution temperature (LCST) type.

LCST-type temperature- responsive polymers have the following characteristics: when the temperature of the solution is lower than the critical solution temperature, the polymer is completely dissolved in the solution; and when the temperature rises above the critical solution temperature, the conformation of the polymer changes from a hydrophilic random coil to a hydrophobic sphere, which will precipitate out of solution and produce a precipitate. The most typical LCST-type polymer is the nitrogen-substituted polyacrylamide polymer. However, when the hydrogen atom on the nitrogen is replaced by a hydrophobic group (such as an alkyl group) and the hydrophobic group is sufficiently hydrophobic (mainly related to the number and type of the substituent), the homopolymer gets the temperature-sensitive features. Poly(*N*-isopropylacrylamide) (PNIPAM) has been widely studied because of its simple preparation, rapid response, and its LCST between 30-32 ^{o}C, which is close to human body temperature. [9] In addition, poly N-vinyl amides, polyoxazolines, polyethers, poly(meth) acrylates, etc., are also LCST-type temperature-responsive polymers.[10] Figure 1.1 shows the structures of solution LCST-type polymers.

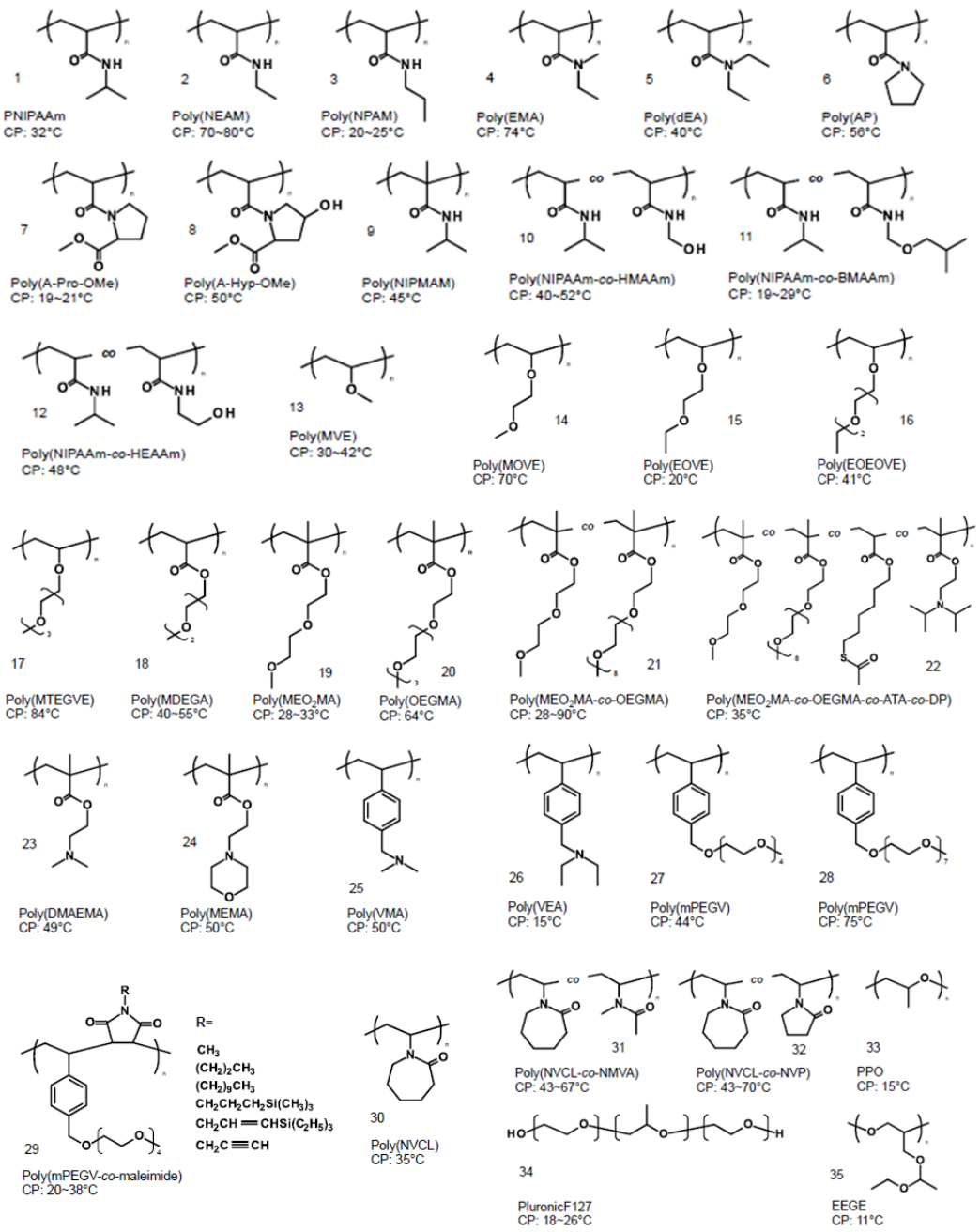

Figure 1.1 *Structures of lower critical solution temperature (LCST) type of thermo-responsive copolymers for dual thermo-responsive block copolymers.*[10]

The UCST-type temperature-responsive polymer exhibits a completely different phase transition behavior than the LCST-type polymer. When the temperature is above

the critical solution temperature, the polymer completely dissolves in a homogeneous phase; and when the temperature is below the critical solution temperature, phase separation occurs and the polymer precipitates out of the solution. Compared with LCST-type polymers, there are fewer types of UCST-type polymers, most of which are amphoteric polyelectrolyte polymers or some urea-containing polymers [10].Figure 1.2 shows the structures of UCST-type polymers and the structures of some dual-thermo-responsive polymer.

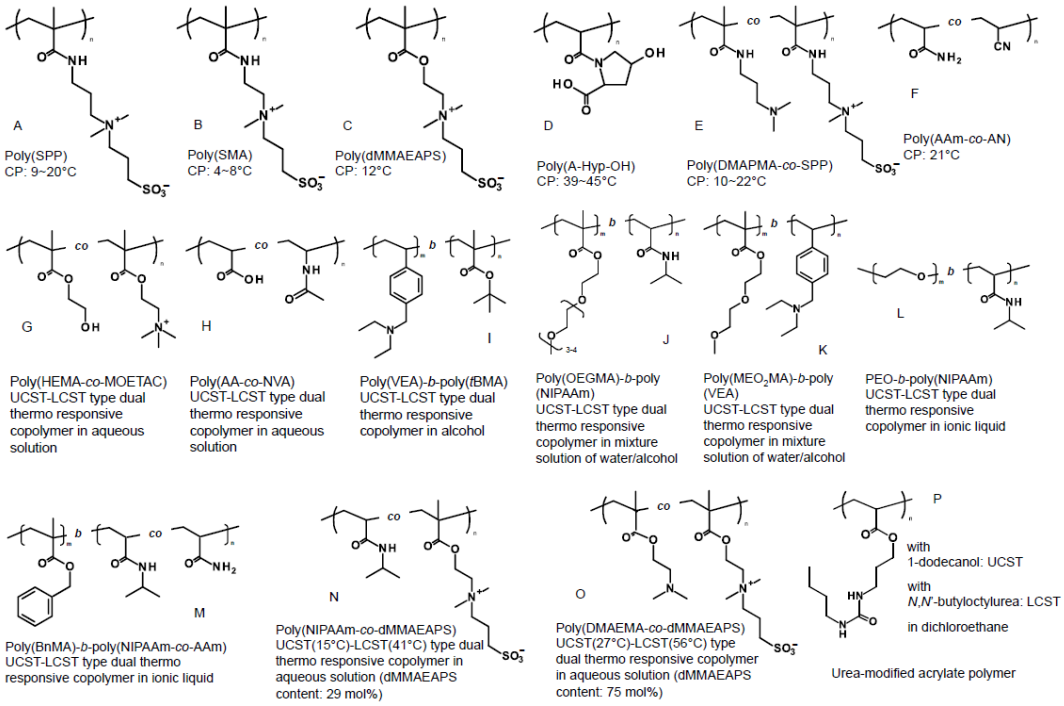

Figure 1.2 *Structures of upper critical solution temperature (LCST) type of thermo-responsive copolymers for dual thermo-responsive block copolymers.* [10]

1.1.1.2 Application of thermo-responsive polymer

The thermo-responsive polymers undergo a change in the hydrophilicity of the segment near the phase transition temperature, thereby changing their solubility. Therefore, they are often used as an intelligent "switch" in many fields. Among them, the most studied areas include biomedicine, chemical and biocatalysis, sensors, and enrichment and separation.

The application of thermo-responsive polymers in biomedical applications mainly includes three aspects: drug delivery, gene transfer and tissue engineering [11-13]. And the most widely used is drug delivery. By using thermo-responsive polymers as drug carriers, the hydrophilicity of the temperature-sensitive polymers can be changed by controlling the temperature, thereby achieving the purpose of controlling the drug release rate.

Thermo-responsive polymers are also used in the field of catalysis. The change of the conformation of the temperature-responsive polymer near the phase transition temperature promotes the aggregation and precipitation of the polymer from the solution to achieve the purpose of catalyst recovery. In addition, the effective area of the catalyst also changes during the process of the polymer changing from the dispersed state to the aggregated state with temperature. So that the catalyst has different catalytic

properties at different temperatures to achieve the purpose of controlling the catalytic activity. [14-18]

The solubility of the thermo-responsive polymer changes greatly as the external temperature changes. Thus, it is possible to utilize this property to prepare the temperature sensors. In addition, they can also be applied to enrichment and separation.

1.1.2 pH-responsive polymer

The size or morphology of the pH-responsive polymers change with the pH, and this change is usually a nonlinear change. The pH sensitive polymers contain a large amount of acid or base groups which are easily hydrolyzed or protonated. With the changes in the pH and ionic strength of the medium, these groups are ionized that causes a change in the ion concentration inside and outside the polymer, and causes hydrogen bond dissociation between the macromolecular segments, and ultimately causes a discontinuous swelling volume change or solubility change. Near the critical pH, the polymer chain undergoes a reversible conformational transition (in some cases accompanied by a phase transition).[19-20]

1.1.2.1 Type of pH-responsive polymer

The pH-responsive polymers that have been reported are very numerous, and they are

roughly classified into two types depending on the electrolyte group. One is an acidic group sensitive type, such as poly (methacrylic) acid (PMAAc), which is an acidic group responsive polymer that accepts protons under acidic conditions and releases protons under neutral or basic conditions. The other is a basic group sensitive type, such as poly(2-dimethylamino)ethyl methacrylate (PDMA), which is a basic group responsive polymer that accepts protons under acidic conditions and forms a positively charged polymer chain.

The acidic groups which can be used to prepare the pH-responsive polymers mainly include four groups: carboxyl group, sulfonic acid group, phosphoric acid group, and boronic acid group. These weakly acidic pendant groups accept protons under acidic conditions and release them under neutral or basic conditions. Their pKa values determine whether they form the polyelectrolytes under acidic or basic conditions. Such ionic or nonionic conversion allows us to adjust their hydrophilicity or hydrophobicity. And this hydrophilic or hydrophobic adjustment changes the state of the polymer chain and causes dissolution or precipitation. The macroscopic phenomenon is that the polymer will swell or dissolve, or the hydrophilic and hydrophobic nature of the polymer surface and particle is altered.

The pH-responsive polymers containing weakly basic groups can be ionized or

deionized at the pH 7 to 11. These basic groups, such as amine group, amide group, morpholinyl group, pyrrolidinyl group, imidazole group, piperazine group, and pyridylgroup, accept protons by forming polyelectrolytes at low pH and release protons under alkaline conditions.

1.1.2.2 Application of pH-responsive polymer

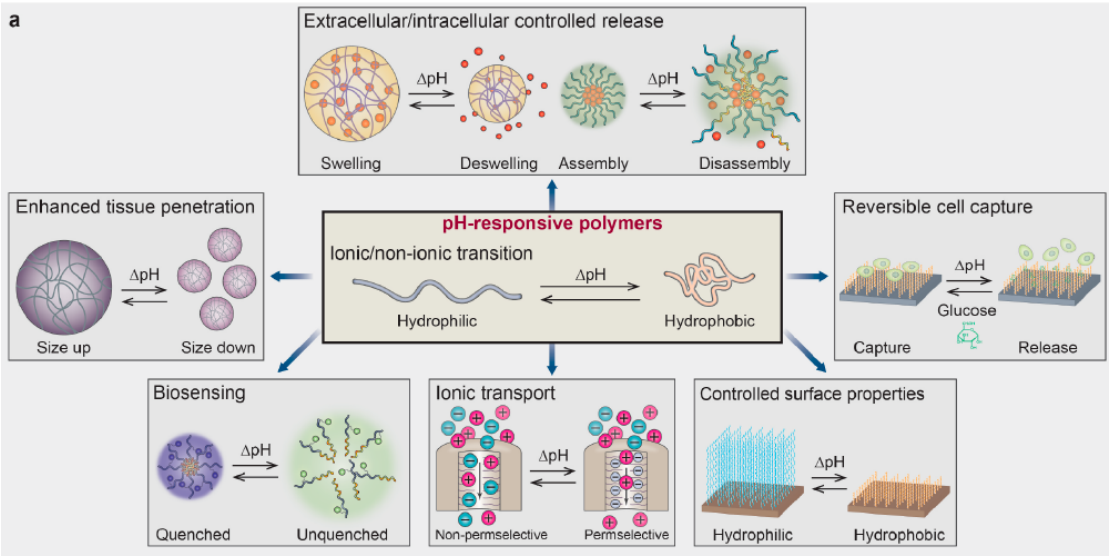

Figure 1.3 *Various applications of pH-responsive polymers and their mechanisms.* [23]

The pH-responsive polymers have high application value in nano reactors, surfactants, imaging photon probes, and targeted drug carriers (Figure 1.3).[21-23]Especially, in the application of pharmaceutical carriers, pH-responsive polymers have great potential. Drugs entering the human body will face complex pH environments. For example, oral

preparations need to undergo an acidic environment of the stomach and then into the neutral and weakly alkaline environment of the intestine; while the anti-tumor drugs need to face an environment where the pH outside the tumor cells (pH=6.8-7.2) and the intracellular inclusion bodies and lysosomes (pH=5-6) are lower than the pH in the surrounding tissues and blood (pH=7.4).[24-26] Loading the drug into the pH-responsive polymer can form a smart drug with controlled release system, which is regulated by the pH environment in the body, and reduce the side effects of the drug.

1.2 Polymer micelle

Polymer micelle is the nanoparticle with a spherical core-shell structure formed by self-assembly of the amphiphilic polymer material in an aqueous environment, and its size is generally between several tens of nanometers and several hundred nanometers. The polymer micelle formed by self-assembly consists of a hydrophilic outer shell and a hydrophobic core, the hydrophilic outer shell can enhance the stability in aqueous solution, and the hydrophobic core can improve the solubility of the poorly soluble drug. Studies have shown that fat-soluble drugs are similarly compatible with the hydrophobic portion of polymer micelles, and like surfactants, drugs are controlled internally. And different from surfactants, polymer micelles often use low toxicity and

biocompatibility materials, which have high research value in drug-loading field. In addition, the nano-size polymer micelles minimize the risk of capillary embolization compared to larger drug carriers. They also avoid renal filtration and reticuloendothelial system (RES) uptake[27].

1.2.1 Type of polymer micelle

According to different basic structural units of self-assembly, polymer micelles can be roughly classified into block copolymer micelles, graft copolymer micelles, and supramolecular micelles.

1.2.1.1 Block copolymer micelle

The block copolymer is obtained by joining two or more polymer chains having different properties. Typical hydrophilic fragments include polyethylene glycol, polyvinyl pyrrolidone, polyoxyethylene, etc., and the hydrophobic fragments include polylactic acid, polycaprolactone, polyglycolic acid and the like. These copolymers with different properties together form a plurality of diblock and triblock amphiphilic polymers. After being suspended in water, these amphiphilic polymers can be self-assembled to form polymer micelles driven by some non-covalent bond forces.

1.2.1.2 Graft copolymer micelle

Graft copolymers are obtained by graft copolymerization of two or more kinds of monomers. If the graft copolymer is composed of a hydrophobic skeleton chain and a hydrophilic branch, the graft copolymer disperses in water and self-assembles to form nanoshells with a core-shell structure, where the core is composed of the hydrophobic skeleton chain and the shell is composed of the hydrophilic branch. Conversely, grafting a hydrophobic side chain on a hydrophilic main chain also gives micelles. The preparation of such a graft copolymer is usually carried out by using a macro-monomer route[28] or by grafting a natural polymer, which can effectively control the configuration of the graft copolymer, the length and number of the branch, and the grafting point. For example, Wang et al[29] grafted a hydrophobic alkyl group onto a linear polyethyleneimine to obtain the polymer micelle with a core-shell structure that the hydrophilic main chain was toward outside and the hydrophobic alkyl chain self-assembled to form the inner core. Chang et al[30] modified sodium alginate with 4-aminobenzenethiol to successfully prepare the amphiphilic thiolated sodium alginate.

1.2.1.3 Supramolecular micelle

Supramolecular micelles with specific function and properties are formed by a

plurality of monomers through the non-covalent bonds. Supramolecular micelles have a number of advantages, such as easy to prepare, safety, low toxicity, etc., and as such, they have a wide range of applications in drug delivery systems. Shi et al[31]constructed a supramolecular polymer micelle based on the electrostatic interaction between hyper-branched polyethyleneimine and hexadecanoic acid, encapsulated metal ions, and reduced by $NaBH_4$ to obtain a blue metal nanopoint chloroform solution.

1.2.2 Stimuli-responsive polymer micelle

Stimuli-responsive polymer micelles, also known as environmentally responsive polymer micelles, are capable of responding quickly to changes in the external environment, leading to changes in their physical and chemical properties and structure. The traditional nano drug carriers cannot effectively control the release of the drug, resulting in an unsatisfactory therapeutic effect. Environmentally responsive micelles as drug carriers first adapt to human environmental conditions. When pH, glutathione, temperature, proton intensity, light intensity, etc. change, they can change according to different mechanisms, and then release the drug to directly kill the bacteria. Or they can be recognized by cancer cells, release drug in cancer cells after being endocytosed, and kill cancer cells to achieve a good therapeutic effect (Figure 1.4).[32] Therefore, the

design of a polymer micelle as the drug carrier requires response to different environmental factors according to the corresponding pathology [33].

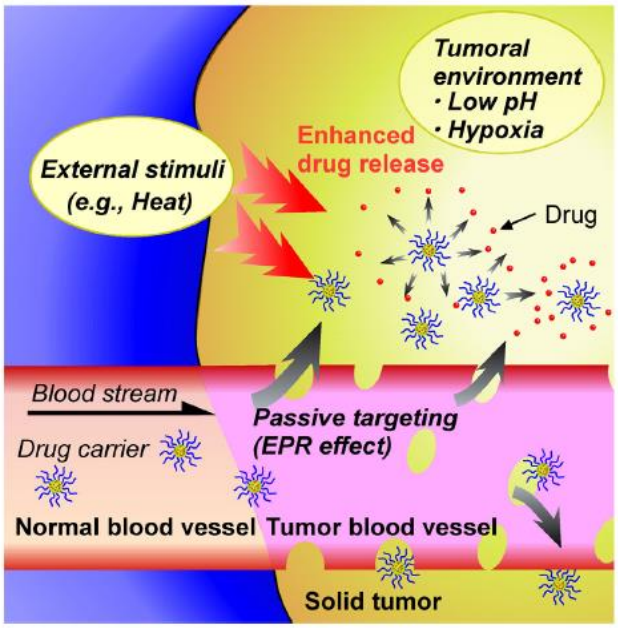

Figure 1.4*Illustration of solid tumor targeting by a stimuli-responsive drug carrier system.* [32]

1.2.2.1 Thermo-responsive polymer micelle

Studies on tumor tissues have found that the temperature of the tumor site (40-45 ^{o}C) is slightly higher than that of normal tissue (37 ^{o}C)[26], so the preparation of thermo-sensitive micelles with thermo-sensitive materials has emerged. Thermo-sensitive polymer micelles utilize the temperature difference between the tumor site and normal tissue to control drug release. Poly (*N*-isopropylacrylamide) is one of the most common temperature sensitive materials for the preparation of thermo-sensitive polymer micelles using in drug carriers (Figure 1.5).[32]

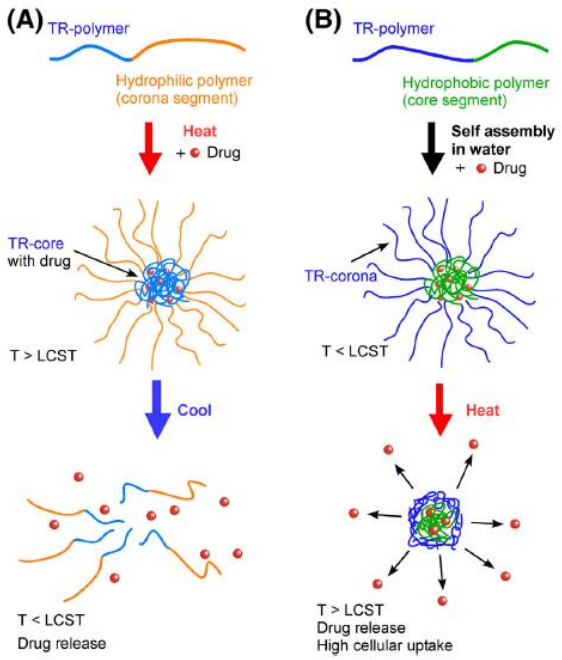

Figure 1.5 *Temperature-responsive (TR) polymeric micelle system using TR polymer as the (A) core or (B) corona segments.*[32]

1.2.2.2 pH-responsive polymer micelle

Due to the abnormal proliferation and metabolism of tumor cells, the oxygen supply to the tumor site is insufficient, so that a large amount of ATP hydrolysate and lactic acid produced by tumor cell metabolism are accumulated in the tumor site, resulting in the pH in the vicinity of the cancer tissue lower than that of the normal cells and the pH in human blood[26]. Because cancer cells are in a weakly acidic environment, research and development of pH-sensitive micelles has attracted more and more researchers' attention. Introducing the pH-sensitive functional group such as amide group, thiol group, or ester group into the block copolymer of micelle, or directly connecting the

drugs with pH-sensitive chemical bonds are the common methods to prepare the pH-sensitive polymer micelles, which can be used as drug carriers and control the drug release. Zhong et al[34]connected the poorly soluble drug doxorubicin to the hydrophobic core of the micelle through the pH-sensitive hydrazone bond. When in a weakly acidic environment, the hydrazone bond is broken and the doxorubicin is released. Li et al[35]designed and synthesized the polymer micelle with a large amount of carboxyl groups in its side chain. In a normal environment, the micelles can carry a large amount of doxorubicin through the electrostatic interaction of the negative charge on the carboxyl group and the positive charge on the doxorubicin. When in a low pH environment, the degree of protonation of the carboxyl group is deepened, so that the electrostatic effect is weakened and the doxorubicin is released (Figure 1.6).[36]

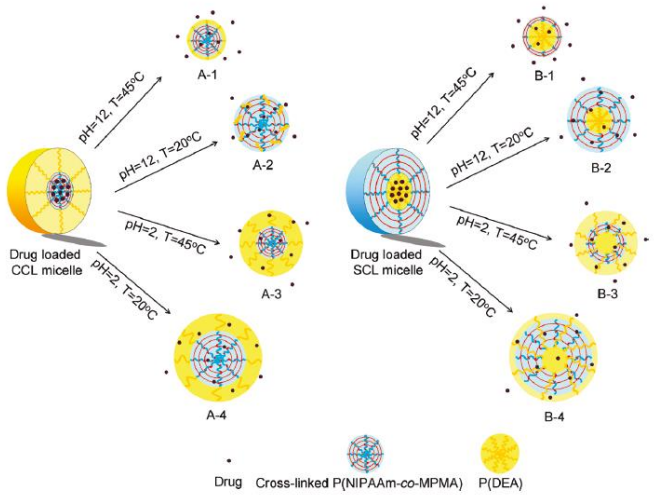

Figure 1.6*Schematic illustration of temperature and pH controlled drug release from CCL and SCL micelles.*[36]

1.2.3 Method for preparing polymer micelle

Common methods for preparing polymer micelles include dialysis, emulsification-volatilization, and thin-film hydration.

1.2.3.1 Dialysis method

In the dialysis method, the polymer micelles are dissolved in a water-miscible organic solvent, and then dialyzed in water or aqueous solution with the dialysis bag to remove the organic solvent to obtain the polymer micelle. Cui et al[37]modified chitosan with polyethylene glycol monomethyl ether to prepare novel chitosan derivatives, and obtained their nanomicelles by dialysis method. Fluorescence spectroscopy and particle size analysis showed that the critical micelle concentration was 0.014 mg/mL, and the average particle size and polydispersity coefficient increased with the increase of sample concentration.

1.2.3.2 Emulsification-volatilization method

In the emulsification-volatilization method, the polymer is first dissolved in a water-insoluble organic solvent such as tetrahydrofuran, and distilled water is added under stirring to form the oil-water phase stratified solution, which has a continuous aqueous phase as an external phase and an organic phase as an internal phase. The

polymers rearrange to form micelles, and finally the organic solvent is removed to obtain the micelle aqueous solution.Dai et al[38] dissolved carboxymethyl chitosan-grafted-polycaprolactone and apatinib in a mixed organic solvent(CH_2Cl_2 and CH_3OH were mixed in proportion, the former dissolved the polymer and the latter dissolved apatinib), and the micelle of carboxymethyl chitosan-grafted-polycaprolactone loaded with apatinib was prepared by emulsification-volatilization method. Subsequent experiments showed that the micelle has good solubilization and good enhanced permeability and retention effect.

1.2.3.3 Thin-film hydration method

In the thin-film hydration method, the polymer is first dissolved in an organic solvent, and then a solid film of the polymer is obtained by volatilization of the solvent, and finally it is added to water to obtain the micelle. In this method, in order to protect the activity of the drug, it is necessary to select a solvent with a lower boiling point. Huang et al[39]prepared the PEG-polylactic acid micelle loaded with vinpocetine through the thin-film hydration method, and optimized the preparation parameters of the micelle with drug loading, encapsulation efficiency and particle size. And the prepared micelle has a drug loading of 20.35% and a particle size of 118.3 nm.

1.3 Protein protection

The synthesis and maintenance of correctly folded proteins are essential processes within all living cells.[40]The accumulation of misfolded or aggregated proteins can lead to cell death or neurodegenerative conditions, such as Parkinson's disease, Alzheimer's disease and Huntington's disease. Figure1.7 shows different aggregation structures of protein.[41-45]Kampinga and his co-workers found that members of the HSPA (HSP70) and DNAJ (HSP40) chaperone families are major mediators of protein quality control. They can recognize misfolded proteins and promote their refolding or degradation in an ATP-dependent manner.[46] However, in clinical phase, these neurodegenerative diseases are still difficult to cure. Therefore, protein aggregation inhibition agent has garnered widespread attention. Various polymers have been reported which exhibit the property of suppression of protein aggregation. Kazushi Kinbaraand his group reported that triangular poly(ethylene glycols) (PEG) analogue show suppression of protein aggregation. In the presence of triangular PEG, nearly 80 % of the lysozyme retain the enzymatic activity.[47]

In our previous study, we synthesized various polysulfobetaine (PSPB) polymers and we found that these polymers can suppress insulin and hen egg-white lysozyme aggregation by acting as a molecular shield. The molecular weight and hydrophobicity

of the polymers effected the ability to suppress of insulin and lysozyme aggregation.[48-50]

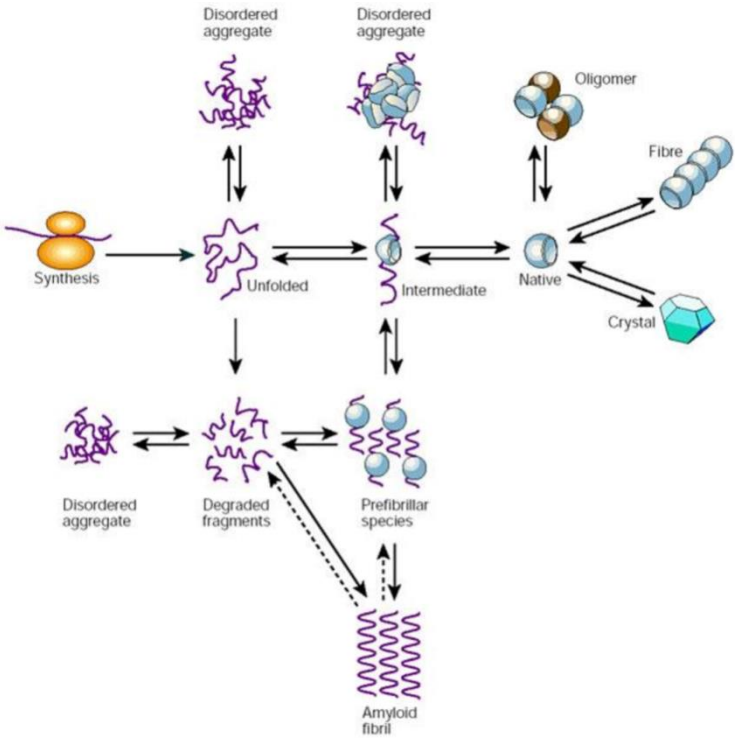

Figure 1.7*A unified view of some of the types of structure that can be formed by polypeptide chains.*[41]

1.4 Research objective

In our group's previous work, we reported that carboxylated ε-poly-l-lysine (COOH-PLL), which was synthesized by introducing succinic anhydride (SA) into ε-poly-l-lysine (PLLSA) exhibit LCST property. However, a single stimuli-responsive polymer can no longer fulfill the demands of the growing industry. Meanwhile, except its use as a cryopreservation agent, not much work has been done to explore the

applications of PLLSA. Therefore, the synthesis of multiple stimuli polymers, which contains PLLSA block, and the development of new applications of the PLLSA is focused on this study. In this study, I have synthesized thermo- and pH-responsive polymers by using different polyampholyte blocks. And the synthesized polymers were used as suppressors of protein aggregation.

Chapter 2: In this chapter, graft copolymers consisting of two different polyampholyte blocks were synthesized via reversible addition fragmentation chain transfer polymerization. These polymers showed dual properties of thermo- and pH-responsiveness in an aqueous solution. Owing to the biocompatible and stimuli-responsive nature of the polymers, this system was shown to effectively release proteins (lysozyme) while simultaneously protecting them against denaturation.

Chapter 3: This chapter describes the synthesis of polymeric micelles and their applications in the drug release systems. Based on the system in chapter 2, I introduced cholesterol into the graft polymers. After the addition of cholesterol, these polymers formed the micelles by self-assembly in an aqueous solution. And these micelles can be used as hydrophobic drug release systems.

Chapter 4: In this chapter, I summarized the work in each chapter above and give the future outlook based on the project which already done above.

1.5 References

(1)Seidi, F.; Jenjob, R.; Crespy, D. Designing Smart Polymer Conjugates for Controlled Release of Payloads. *Chem. Rev.***2018**, *118*, 3965−4036.

(2)Anamica; Pande, P.P. An Overview on Smart pH Responsive Polymers. *Asian J. Chem.***2018**, *30*, 711-718.

(3) Liu, F.; Urban, M. W. Recent Advances and Challenges in Designing Stimuli-responsive Polymers. *Prog.Polym.Sci.***2010**, *35*, 3-23.

(4)Zhang, Q.; Vancoillie, G.; Mees, M. A.; Hoogenboom, R. Thermoresponsive Polymeric Temperature Sensors with Broad Sensing Regimes. *Polym. Chem.***2015**, *6*, 2396-2400.

(5) Singh, N. K.; Lee, D.S. In Situ Gelling pH- and Temperature-sensitive Biodegradable Block Copolymer Hydrogels for Drug Delivery. *J. Controlled Release***2014**, *193*, 214-227.

(6)Lin, W.; Yao, N.; Qian, L.; Zhang, X.; Chen, Q.; Wang, J.; Zhang, L. pH-responsive Unimolecular Micelle-gold Nanoparticles-drug Nanohybrid System for Cancer Theranostics. *ActaBiomater.***2017**, *58*, 455-465.

(7)Stuart, M. A. C.; Huck, W. T. S.; Genzer, J.; Marcus, M.; Christopher, O. Emerging

Applications of Stimuli-responsive Polymer Materials[J]. *Nat.Mater.***2010**, *9*, 101.

(8)Weber, C.; Hoogenboom, R.; Schubert, U. S. Temperature Responsive Bio-compatible Polymers Based on Poly (ethylene oxide) and Poly (2-oxazoline) s. *Prog.Polym.Sci.***2012**, *37*, 686-714.

(9) Yang, W.; Tang, Z.; Luan, Y.; Liu, W.; Li, D.; Chen, H. Thermo-responsive Copolymer Decorated Surface Enables Controlling the Adsorption of a Target Protein in Plasma. *ACS Appl. Mater. Interfaces***2014**, *6*, 10146-10152.

(10)Kotsuchibashi, Y.; Ebara, M.; Aoyagi, T.; Narain, R. Recent Advances in Dual Temperature Responsive Block Copolymers and Their Potential as Biomedical Applications. *Polymers***2016**, *8*, 380.

(11)Cobo, I.; Li, M.; Sumerlin, B. S.; Perrier, S. Smart Hybrid Materials by Conjugation of Responsive Polymers to Biomacromolecules. *Nat.Mater.***2015**, *14*, 143.

(12) Ward, M. A.; Georgiou, T. K. Thermoresponsive Polymers for Biomedical Applications. *Polymers***2011**, *3*, 1215-1242.

(13) Yang, K.; Wan, S.; Chen, B.; Gao, W.; Chen, J.; Liu, M.; He, B.; Wu, H. Dual pH and Temperature Responsive Hydrogels Based on β-cyclodextrin Derivatives for Atorvastatin Delivery. *Carbohyd.Polym.***2016**, *136*, 300-306.

(14) Qi, J.; Lv, W.; Zhang, G.; Li, Y.; Zhang, G.; Zhang, F.; Fan, X. A Graphene-based

Smart Catalytic System with Superior Catalytic Performances and Temperature Responsive Catalytic Behaviors.*Nanoscale***2013**, *5*, 6275-6279.

(15) Dong, Y.; Wang, Q.; Wang, J.; Ma, Y.; Wang, D.; Wu, Z.; Abudkremb, M.; Zhang,M. Temperature Responsive Copolymer as Support for Metal Nanoparticle Catalyst: A Recyclable Catalytic System. *React.Funct.Polym.***2017**, *112*, 60-67.

(16) Xu, Z.; Uddin, K. M. A.; Ye, L. Boronic Acid Terminated Thermo-responsive and Fluorogenic Polymer: Controlling Polymer Architecture for Chemical Sensing and Affinity Separation. *Macromolecules*, **2012**, *45*, 6464-6470.

(17) Liu, G.; Wang, D.; Zhou, F.; Liu, W. Electrostatic Self-Assembly of Au Nanoparticles onto Thermosensitive Magnetic Core-Shell Microgels for Thermally Tunable and Magnetically Recyclable Catalysis. *Small***2015**, *11*, 2807-2816.

(18) Chen, J.; Xiao, P.; Gu, J.; Han, D.; Zhang, J.; Sun, A.; Wang, W.; Chen, T. A Smart Hybrid System of Au Nanoparticle Immobilized PDMAEMA Brushes for Thermally Adjustable Catalysis. *Chem.Commun.***2014**, *50*, 1212-1214.

(19)Gil, E. S.; Hudson, S. M.Stimuli-reponsivePolymers and Their Bioconjugates. *Prog. Polym. Sci.***2004**, *29*, 1173-1222.

(20)Rodríguez-Hernández, J.; Chécot, F.; Gnanou, Y.; Lecommandoux, S.Toward 'Smart' Nano-objects by Self-assembly of Block Copolymers in Solution. *Prog. Polym.*

Sci.**2005**, *30*, 691-724.

(21) Chen, J.K.; Chang, C. J. Fabrications and Applications of Stimulus-responsive Polymer Films and Patterns on Surfaces: A Review. *Materials***2014**, *7*, 805-875.

(22)Lee, Y.; Fukushima, S.; Bae, Y.;et al. A Protein Nanocarrier from Charge-conversion Polymer in Response to Endosomal pH. *J. Am. Chem. Soc*.**2007**, 129, 5362-5363.

(23)Tao, W.; Wang, J.; Parak, W. J.; Farokhzad, O. C.; Shi, J. Nanobuffering of pH-Responsive Polymers: A Known but Sometimes Over looked Phenomenon and Its Biological Applications. *ACS Nano***2019**, *13*, 4876−4882.

(24)Rofstad, E.K.; Mathiesen, B.;Kindem, K.; Galappathi, K. Acidic Extracellular pH Promotes Experimental Metastasis of Human Melanoma Cells in Athymic Nude Mice. *Cancer Res.***2006**, *66*, 6699-6707.

(25)Dissemond, J.; Witthoff, M.; Brauns, T. C.; Haberer, D.; Goos, M. pH Values in Chronic Wounds: Evaluation During Modern Wound Therapy. *Der Hautarzt***2003**, *54*, 959-965.

(26)Vaupel, P.; Kallinowski, F.; Okunieff, P. Blood Flow, Oxygen and Nutrient Supply, and Metabolic Microenvironment of Human Tumors: A Review. *Cancer Res.***1989**, *49*, 6449-6465.

(27)Kataoka, K.; Kwon, G. S.; Yokoyama, M.;Okano, T.; Sakurai, Y. Block-copolymer Micelles as Vehicles for Drug Delivery. *J. Control. Release*, **1993**, *24*, 119-132.

(28)Jeong, J. H.; Park, T. G. Poly(L-lysine)-g-poly(D,L-lactic-co-glycolic acid) Micelles for Low Cytotoxic Siodegradable Gene Delivery Carriers. *J. Control. Release***2002**, *82*, 159-166.

(29)Wang, W.; Qu, X.; Gray, A. I.; Tetley, L.; Uchegbu, I. F. Self-assembly of Getyl Linear Polyethylenimine to Give Micelles, Vesicles, and Dense Nanoparticles. *Macromolecules***2004**, *37*, 9114-9122.

(30)Zheng, X. L.; Kan, B.; Gou, M. L.; Fu, S. Z.; Zhang, J.; Men, K.; Chen, L. J.; Luo, F.; Zhao, Y. L.; Zhao, X.; Wei, Y. Q.; Qian, Z. Y. Preparation of MPEG-PLA Nanoparticle for Honokiol Delivery in Vitro. *Int. J. Pharm.***2010**, *386*, 262-267.

(31) Shi, Y.; Tu, C.; Wang, R.; Wu, J.; Zhu, X.; Yan, D. Preparation of CdS Nanocrystals within Supramolecular Self-Assembled Nanoreactors and Their Phase Transfer Behavior. *Langmuir* **2008**, *24*, 11955-11958

(32)Akimoto, J.; Nakayama, M.; Okano, T. Temperature-responsive Polymeric Micelles for Optimizing Drug Targeting to Solid Tumors. *J. Control. Release***2014**, 193, 2-8.

(33)Hunt, C. A.; Macgregor, R. D.; Siegel, R. A. Engineering Targeted in Vivo Drug Delivery. I. The Physiological and Physicochemical Principles Governing Opportunities

and Limitations. *Pharm. Res. Dordr.***1986**, *3*, 333-344.

(34) Zhou, L.; Cheng, R.; Tao, H.; Ma, S.; Guo, W.; Meng, F.; Liu, H.; Liu, Z.; Zhong, Z. Endosomal pH-Activatable Poly(ethylene oxide)-*graft*-Doxorubicin Prodrugs: Synthesis, Drug Release, and Biodistribution in Tumor-Bearing Mice.*Biomacromolecules***2011**, *12*, 1460-1467.

(35)Li, M.; Lv, S.; Tang, Z.; Song, W.; Yu, H.; Sun, H.; Liu, H.; Chen, X. Polypeptide/Doxorubicin Hydrochloride Polymersomes Prepared Through Organic Solvent-free Technique as a Smart Drug Delivery Platform. *Macromol.Biosci.***2013**, *13*, 1150-1162.

(36) Chang, C.; Wei, H.; Feng, J.; Wang, Z. C.; Wu, X., J.; Wu, D. Q.; Cheng, S. X.; Zhang, X. Z.; Zhuo, R. X. Temperature and pH Double Responsive Hybrid Cross-Linked Micelles Based on P(NIPAAm-co-MPMA)-b-P(DEA): RAFT Synthesis and “Schizophrenic” Micellization. *Macromolecules***2009**, *42*, 4838-4844.

(37) Cui, J.; Huang, K.; Ma, L.; Tu, M.; Liu, H.; Yan, Y.; Qin, C. Study on Self-Assembled Nano-Micelles Based on Poly(Ethylene Glycol)-Grafte Chitosan. *J Hubei Eng. Univ.***2014**, *34*, 20-24.

(38) Dai, Y. X.; Lang, M. D. Preparation and Sustained Release of Carboxymethyl Chitosan Derived Micelles. *J. Funct. Polym.***2018**, 31, 75-81.

(39) Huang, Z. J.; Li, T.; Guo, X. J.; Wang, Y. T.; Yang, M. Q.; Huang, S. L.; Yang, F.; Wu, Y. L.; Dian, S. N. Technical Study of Vinpocetine Micelles Prepared by Thin-film Hydration Method. *Chin. Med. Mat.***2012**, *35*, 1850-1851.

(40) Labbadia, J.; Novoselov, S. S.; Bett, J. S.; Weiss, A.; Paganetti, P.; Bates, G. P.; Cheetham, M. E. Suppression of Protein Aggregation by Chaperone Modification of High Molecular Weight Complexes. *Brain***2012**, *135* (4), 1180–1186.

(41) Wei Wang. Instability, Stabilization, and Formulation of Liquid Protein *Pharmaceuticals*; **1999**, 185, 129-188.

(42) Ross, C. A.; Poirier, M. A. Protein Aggregation and Neurodegenerative Disease. *Nat. Med.***2004**, *10* (7), S10.

(43) Chiti, F.; Dobson, C. M. Protein Misfolding, Functional Amyloid, and Human Disease. *Annu. Rev. Biochem.***2006**, *75* (1), 333–366.

(44) Peter T. Lansbury & Hilal A. Lashue. A Century-Old Debate on Protein Aggregation and Neurodegeneration Enters the Clini. *Nature,***2006**, *443*, 774–779.

(45) Edwad H. Koo, Peter T. Lansbury, JR., Jeffery W. Kelly. Amyloid Diseases: Abnormal Protein Aggregation in Neurodegeneration. *Proc. Natl. Acad. Sci.* **1999**, *96* (1), 9989–9990.

(46) Harm H. Kampinga and Elizabeth A. Craig. The Hsp70 Chaperone Machinery:

J-Proteins as Drivers of Functional Specificity. *Nat Rev Mol Cell Biol.***2010**, *11* (8), 579–592.

(47)Muraoka, T.; Adachi, K.; Ui, M.; Kawasaki, S.; Sadhukhan, N.; Obara, H.; Tochio, H.; Shirakawa, M.; Kinbara, K. A Structured Monodisperse PEG for the Effective Suppression of Protein Aggregation. *Angew. Chemie - Int. Ed.***2013**, *52* (9), 2430–2434.

(48) Rajan, R.; Matsumura, K. Inhibition of Protein Aggregation by Zwitterionic Polymer-Based Core-Shell Nanogels. *Sci. Rep.***2017**, *7*, 1–9.

(49) Rajan, R.; Suzuki, Y.; Matsumura, K. Zwitterionic Polymer Design That Inhibits Aggregation and Facilitates Insulin Refolding : Mechanistic Insights and Importance of Hydrophobicity. *Macromol. Biosci.***2018**, *1800016*, 1–6.

(50) Sharma, N.; Rajan, R.; Makhaik, S.; Matsumura, K. Comparative Study of Protein Aggregation Arrest by Zwitterionic Polysulfobetaines: Using Contrasting Raft Agents. *ACS Omega***2019**, *4* (7), 12186–12193.

Chapter 2

Dual Thermo- and pH-responsive Behavior of Double Zwitterionic Graft Copolymers for Suppression of Protein Aggregation and Protein Release

2.1 Introduction

Stimuli-responsive polymers have attracted great attention in recent years. They respond to small changes in the surrounding environment, which makes them suitable candidates for applications in nanotechnology and biomedicine, for use as drug carriers[1–5] and smart surfaces,[6–9] and for protein separation.[10,11] However, as the field of applications expands, a single stimuli-responsive polymer can no longer fulfil the demands of the growing industry.[12] Therefore, the synthesis of multi-stimuli-responsive polymers has become necessary. Compared with single-stimuli-responsive polymers, multi-stimuli-responsive polymers have additional properties that not only widen the

applicability of polymers, but also allow for better control over the polymer conformation.[13]

Among the various stimuli-responsive polymers reported to date, thermo- and pH-responsive polymers have attracted the most attention.[12, 14] Thermo-responsive polymers can be classified into two types: systems exhibiting lower critical solution temperature (LCST)[15] and upper critical solution temperature (UCST) phase separations. Further, pH-responsive polymers have gained relevance because there is a difference in pH between human organs, normal tissue, and diseased tissue (e.g., the stomach, normal tissue, and a tumor have pH values of 1–2, 7.4, ~6.5, respectively).[16] pH-responsive polymer systems can be developed as drug delivery systems and gene delivery systems in vivo.

Therefore, in this study, we focused on the synthesis of graft copolymers that exhibit dual-thermo- and pH-responsive properties and attempted to control the phase transition temperature by changing the molecular mass and the concentration of the polymers.

For dual-thermo-responsive copolymers, the Poly (*N*-isopropylacrylamide)-poly-sulfobetaine (PNIPAM-PSPB) system has been widely studied. For instance, in our previous research[17], we showed that nanogels made of a copolymer of NIPAM and SPB show dual thermo-responsive reversible properties and

exhibit swelling and shrinking with changing temperature. Additionally, Papadakis and his group reported a series of studies on the relationship between temperature and the shape of PNIPAM-PSPB micelles.[18–20]It is well known that PNIPAM shows LCST, and its transition temperature is observed near the physiological temperature. However, PNIPAM has several shortcomings, including non-biodegradability, inflammation, and activation of platelets when it makes contact with blood.[21, 22] Moreover, the LCST is independent of the molar mass and concentration of the polymer, thus limiting the tunability of its properties by molecular design.[23] Further, PNIPAM does not exhibit a pH-responsive property, owing to its lack of ionic groups.

In a previous work, we reported that poly-L-lysine (PLL)-based polyampholyte, COOH-PLL, shows an LCST type of phase separation, which can be easily controlled by molecular design.[24] PLL is extensively used as a food additive due to its low toxicity.[25] Moreover, PLL can be degraded by amidases.[26] When the NH_2 group of PLL reacts with anhydrides such as succinic anhydride (SA), PLL transforms into an ampholyte molecule with both cationic and anionic moieties and thus exhibits both LCST and pH-responsive properties. Moreover, the LCST behavior can be easily tuned by optimizing charge balance, hydrophobicity, polymer concentration, and so on. Interestingly, COOH-PLL shows excellent cryoprotective properties[27] with various cells.

Furthermore, it has been reported that polyampholyte exhibits anti-biofouling properties.[28, 29] In addition, hydrophobically modified poly-L-lysine polyampholyte has been shown to deliver proteins at low temperatures.[30]

Unlike LCST, UCST has not been reported to occur in many polymers. Among the polymers showing UCST, poly-sulfobetaine (PSPB) has been frequently used. The UCST behavior of PSPB was found to be highly dependent on the molar mass and the concentration of the added low-molar-mass salts.[19] Because of its unique chain structures and high biocompatibility,[31] PSPB has been associated with unique properties such as cryopreservation[32] and has been used for anti-bio adherent coatings.[33] Moreover, in a previous work, we found that this polyampholyte exhibits a protein aggregation inhibition property, owing to its weak and reversible interaction with protein molecules, thereby acting as a molecular shield.[34–36] This phenomenon enables PSPB to assist proteins in the retention of their secondary structures and suppresses fibrillation of the protein, even under severe stress. To utilize this kind of dual thermo-responsive polymer for biomedical applications such as protein delivery, PSPB was chosen along with COOH-PLL in this study for the graft polymer system.

The use of functional proteins in disease therapy has a long history. However, the development of protein therapeutics is limited, owing to protein instability. The

misfolding and aggregation of the therapeutic protein reduces its treatment efficiency and even causes adverse reactions. For the advancement of the protein biopharmaceutics field, the development of newer systems that can protect proteins from unfolding and denaturation during delivery transport or under stress is of paramount importance. Moreover, the development of controlled and triggered release systems has caught the attention of researchers worldwide. In this work, we used reversible addition fragmentation chain transfer (RAFT) polymerization to develop graft copolymers consisting of two zwitterionic blocks, i.e., PLLSA-g-PSPB. The presence of the PLLSA segment allows these graft copolymers to exhibit LCST and pH-responsive properties and the PSPB block allows for UCST-type transition. Furthermore, we studied the phase behavior of these graft copolymers at different temperatures and pH values. Then, because of their pH-responsive properties, we used these graft copolymers as a protein release vehicle.[37]Electrostatic interaction provides a weak and reversible bond between the polymer and protein. Previous reports have suggested that polymer-protein hybrids can also be formed in such systems by self-assembly in aqueous solution.[38–45]Due to the presence of PSPB, the proteins were efficiently protected, even under severe conditions. To the best of our knowledge, the PLLSA-g-PSPB system proposed in this study, which consists of two different ampholytic segments and shows both dual thermo- and

pH-responsive properties, is the first such system. Furthermore, the ability of the system to suppress protein aggregation and help proteins retain their secondary structures is noteworthy.

2.2 Materials and methods

2.2.1 Materials

Sulfobetaine monomer was donated by Osaka Organic Chemical Ind., Ltd. (Osaka, Japan) and used without further purification. A 25% (w/w) ε-poly-L-lysine (PLL) (molecular weight 4000) aqueous solution was purchased from JNC Corp. (Tokyo, Japan). Succinic anhydride (SA), 1-ethyl-3-(3-dimethylaminopropyl) carbodiimide hydrochloride (EDC-HCl) and N-Hydroxysuccinimide (NHS) were purchased from Wako Pure Chemical Ind., Ltd. (Osaka, Japan). 2-(dodecylthiocarbonothioylthio)-2-methylpropinic acid (RAFT agent), 4,4'-azobis-(4-cyanovaleric acid) (V-501, initiator), Thioflavin T (ThT), Micrococcus lysodeikticus and lysozyme from chicken egg white were purchased from Sigma-Aldrich (St. Louis, MO).

2.2.2 Synthesis of carboxylated poly-l-lysine (PLL-SA)

PLL-SA with two different substitutions was synthesized. PLL-SA in which 50 mol% and 65 mol% of the amino groups were converted into COOH by the addition of SA were denoted as PLLSA50 (neutral at pH 7) and PLLSA65 (negative at pH 7), respectively. PLLSA50 was synthesized by adding succinic anhydride (9.76 mmol) to the 25% (w/w) ε-poly-l-lysine (PLL) aqueous solution (10 ml), followed by stirring at 50 °C for 1 h. Similarly, PLLSA65 was synthesized by dissolving succinic anhydride (12.67 mmol) in the 25% (w/w) ε-poly-l-lysine (PLL) aqueous solution (10 ml) followed by stirring at 50 °C for 1 h. After the reaction, the products were dried in an oven overnight and vacuum-dried for 1 day.

2.2.3 Synthesis of Macro-CTA (PLLSA-RAFT agent)

We prepared two types of macro-CTA (PLLSA-RAFT agent): PLLSA50-RAFT agent and PLLSA65-RAFT agent. EDC (0.043 mmol), NHS (0.043 mmol), 2-(dodecylthiocarbonothioylthio)-2-methylpropionic acid (0.011 mmol) and 5 mL DMSO were added to a vial and stirred at 80 °C for 2 h. In another vial, 0.33 mmol PLLSA50 or PLLSA65 was dissolved in 10 mL DMSO at 130 °C. After 2 h, the two solutions were mixed together and reacted at 130 °C for 24 h. The polymer was purified

by dialysis against water for 3 d using a dialysis membrane (MWCO 3.5 KDa, Repligen Corp. Waltham, MA, US). After dialysis, the polymer was obtained by lyophilization.

2.2.4 Synthesis of a graft copolymer of PLLSA and SPB (PLLSA-g-PSPB)

The graft copolymers were synthesized using the following mixture ratio: [SPB monomer]:[V-501]:[macro-CTA] = 1000:1:5. PLLSA50-b-PSPB and PLLSA65-b-PSPB were synthesized by dissolving the SPB monomer (6.6 mmol), V-501 (6.6 μmol), and Macro-CTA (PLLSA50-RAFT and PLLSA65-RAFT agents, respectively) (33 μmol) in water (45 mL). The mixture was purged with nitrogen gas for 1 h and then stirred at 70 °C for 24 h. To study the kinetics of this reaction, the samples were removed from the reaction mixture at regular intervals, and ^{1}H NMR was used to monitor the disappearance of alkene protons during the course of the reaction. The polymer was then purified by dialysis against water for 3 d using a dialysis membrane (MWCO 14 KDa). After dialysis, the polymer was obtained by lyophilization.

2.2.5 Polymer characterization

The structural analyses of all polymer structures and time-dependent NMR were conducted on a 400 MHz Bruker Avance III spectrometer. The data was analyzed by

NMR using the Topspin 3.5 software. The number of repeating units of the graft copolymers was estimated by ^{1}H NMR from the relative area of the two peaks at around 4 ppm (corresponding to the α-protons of the substituted and unsubstituted PLL repeating units) and that of the poly-SPB peak at around 2.2 ppm. The numbers of NH_2 groups were determined by a 2,4,6-trinitrobenzene sulfonic acid (TNBS) assay.[46] In the TNBS assay, glycine was used as the standard solution. A solution containing 0.3 ml of 250 μg/mL of solution, 1 mL 0.1% (w/v) of TNBS solution, and 2 ml of a solution containing 4% (w/v) $NaHCO_3$ and 10% (w/v) sodium dodecylsulfate was prepared. The solution was then incubated at 37 °C for 2 h. After the incubation, the absorbance of the sample solutions was measured at 335 nm using UV-vis spectroscopy (UV-1800, Shimadzu Corp., Kyoto, Japan).

2.2.6 Dynamic light scattering (DLS)

A Zetasizer 300 system (Malvern Instruments, Worcestershire, UK) was used to determine the hydrodynamic diameter and the surface charge of the graft copolymers. The scattering angle was 173°. The thermo-responsiveness of the polymers was measured by DLS in temperature steps of 2 °C with three measurements per temperature.

2.2.7 Ultraviolet–visible (UV-Vis) spectroscopy for the determination of thermo- and pH- responsive properties

The turbidity of the graft copolymers was determined by UV-visible spectroscopy (UV-1800, Shimadzu Corp., Kyoto, Japan) at 550 nm. Each transmittance value was obtained at a different temperature, and there was a 12 min stabilization period at every temperature.

2.2.9 Protein release experiment

A polymer solution (6% (w/w)) and lysozyme solution (2% (w/w)) were prepared in phosphate-buffered saline (PBS, pH 7.4). Following this, the polymer and lysozyme solutions were mixed and incubated for 2 h at 25 °C. After the incubation, the samples were centrifuged for 2 h at 13.2 × 1000 rpm (15 °C) using 30K MWCO centrifugal filter devices. The solution was separated into two parts. A PBS solution appeared in the filtrate collection tube with the non-bound lysozyme, whereas the protein that succeeded in binding with the polymer remained in the filter device. The liquid that appeared in the filtrate collection tube was checked for the non-bound lysozyme by the Bradford assay.[47] Lysozyme loading efficiency was calculated using the following equation.

Protein loading efficiency = (1)

The concentrated solution containing polymer-bound protein, which was retained in the filter device, was diluted, and the pH was reduced to 3 by the addition of 1 M HCl solution. DLS was employed to measure the hydrodynamic radius of the polymer and that of the protein before and after the pH change.

2.2.10 Residual lysozyme activity

A lysozyme solution (20 μM) was mixed with polymer solutions (at various concentrations) in PBS (pH 7.4). Following this, the lysozyme-polymer solution was heated at 90 °C for 30 min. After 30 min, a Micrococcus lysodeikticus (2 mL, 0.25 mg/mL in PBS) solution was mixed with 100 μL of the lysozyme-polymer solution. The transmittance of this mixture solution was measured by UV-vis spectrophotometry (UV-1800, Shimadzu) at 600 nm from 0 to 6 min with constant stirring. A continuous downward line was obtained. The slope of this line indicated the activity of the residual lysozyme.

2.2.11 Fibril formation of lysozyme

The fibril formation of the lysozyme after heating for 30 min at 90 °C was determined by a ThT assay. ThT binds to β-amyloid fibrils, which leads to an increase

in fluorescence intensity.[48] First, the stock solution was prepared by adding 4 mg ThT to a 5 mL PBS solution (pH 7.4) followed by filtration with 0.22 μM filter. Following this, the working solution was prepared by adding 1 mL of the stock solution to 49 mL of PBS (pH 7.4). The lysozyme solution (40 μM) was mixed with an equal volume of the polymer solution. The lysozyme-polymer solution was then heated at 90 °C for 30 min with the final concentration of lysozyme being 20 μM and that of polymer being 1 %, 2.5 %, and 5 % (w/w). Following this, 100 μL of the lysozyme polymer solution was mixed with 2 mL of the ThT solution, and the fluorescence was measured by JASCO FP-8600 with an excitation wavelength of 450 nm and emission wavelength of 485 nm.

2.2.12 Circular dichroism (CD) spectroscopy

A CD spectropolarimeter (JASCO-820) was employed to monitor and determine the change in the secondary structures of the lysozyme before and after heating. A transparent quartz cuvette with a path length of 0.5 cm was used to measure the CD spectra. The final concentration of the lysozyme and polymer components in the lysozyme-polymer solution was 20 μM and 5 % w/w, respectively. The scanning range was 190–320 nm with a bandwidth of 1 nm and scanning speed of 0.2 nm/s.

2.2.13 Cytotoxicity Study

L929 (American Type Culture Collection, Manassas, VA, USA) cells were cultured in Dulbecco's modified Eagle's medium (DMEM, Sigma-Aldrich, St. Louis, MO), supplemented with 10% heat-inactivated fetal bovine serum in a humidified atmosphere of 5% CO_2 at 37 °C. The cytotoxicity assay was performed according to the MTT method in a 96-well plate. Briefly, 1×10^3 cells in 0.1 mL of culture media were seeded in a 96-well plate. After incubation for 72 h, 0.1 mL of the culture medium, which contained different concentrations of the polymer, was added to the 96-well plate. After re-incubation for 24 h, 0.1 mL MTT (3-(4,5-dimethylthiazole-2-yl)-2,5-diphenyltetrazolium bromide) solution (300 μg/mL) was added to each well, and the cells were incubated for an additional 3 h. After discarding the media, 0.1 mL of DMSO was added to dissolve the purple formazan crystals that had formed. The absorbance values at 540 nm were determined using a microplate reader (versa max, Molecular Devices Co., CA, USA). The value of the absorbance indicated the number of viable cells.

2.3 Results and discussion

2.3.1 Polymer characterization

The graft copolymers were prepared by RAFT polymerization as shown in **Scheme 2.1.** Two graft copolymers with different degrees of substitution of SA in PLL were obtained. ^{1}H NMR and ^{13}C NMR spectroscopy were employed to characterize these polymers. We can clearly identify the characteristic peaks of the two segments in Figure 2.1. The degree of substitution (DS) of SA into PLL and the number of RAFT agents substituted per chain were determined by ^{1}H NMR (Figures 2.1and2.2) and the TNBS assay. The obtained degree of substitution of SA was almost the same in the feeding condition (Table 2.1). Calculations based on the results of the TNBS assay and NMR spectroscopy clearly reveal that approximately 1 RAFT agent was substituted on the PLLSA chain (Table 2.1). Table 2.2 shows the molecular weights (M_n) of these polymers, which were calculated by NMR spectroscopy. P1 and P2 represent the copolymers PLLSA(50)-g-PSPB(200) and PLLSA(65)-g-PSPB(200), respectively. Here, 200 in the parenthesis after PSPB indicates the number of repeating units of SPB. The degree of polymerization of SPB in P2 was higher than that of P1. Figures 2.3–2.6 show the ^{1}H- and ^{13}C-NMR charts for P1 and P2.

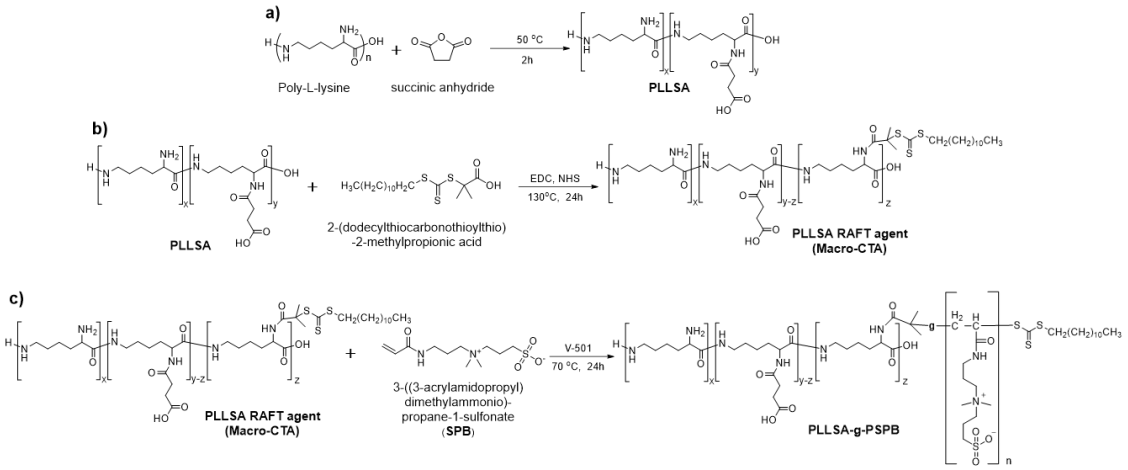

Scheme 2.1 *Schematic illustration of the synthesis of PLLSA-g-PSPB.*

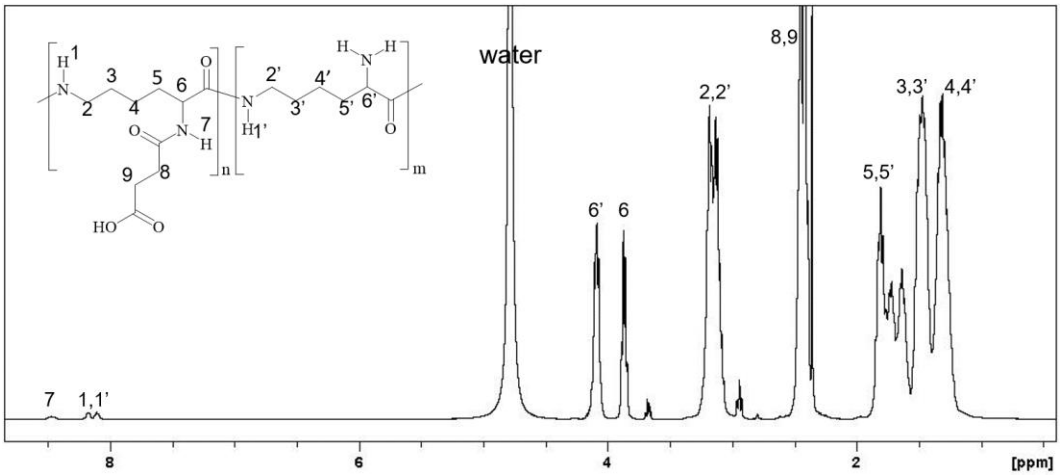

Figure 2.1 *^{1}H NMR of PLLSA in D_2O.*

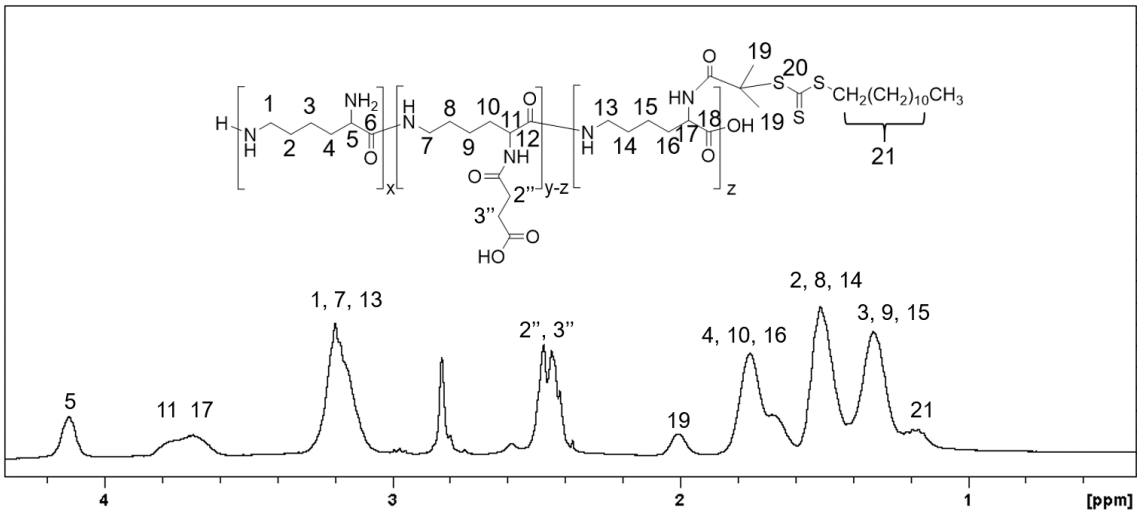

Figure 2.2 *^{1}H NMR of Macro-CTA in D_2O.*

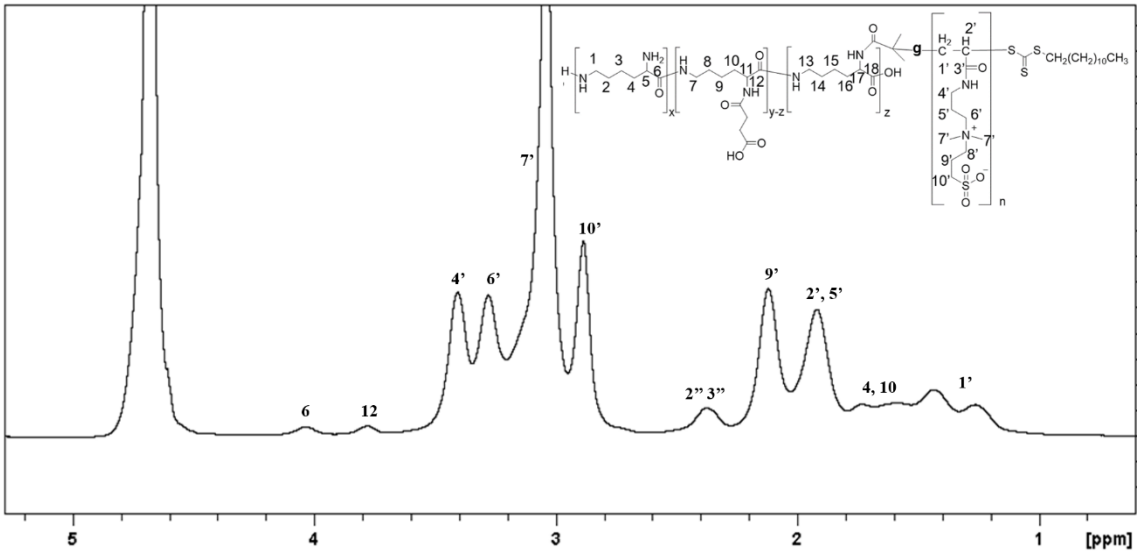

***Figure 2.3**^{1}H NMR of P1in D_2O.*

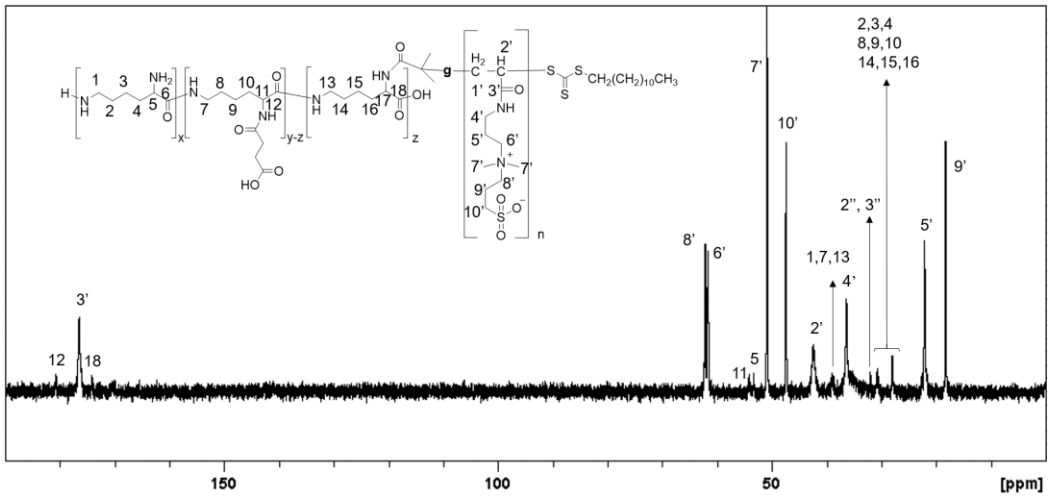

***Figure 2.4**^{13}C NMR of P1in D_2O.*

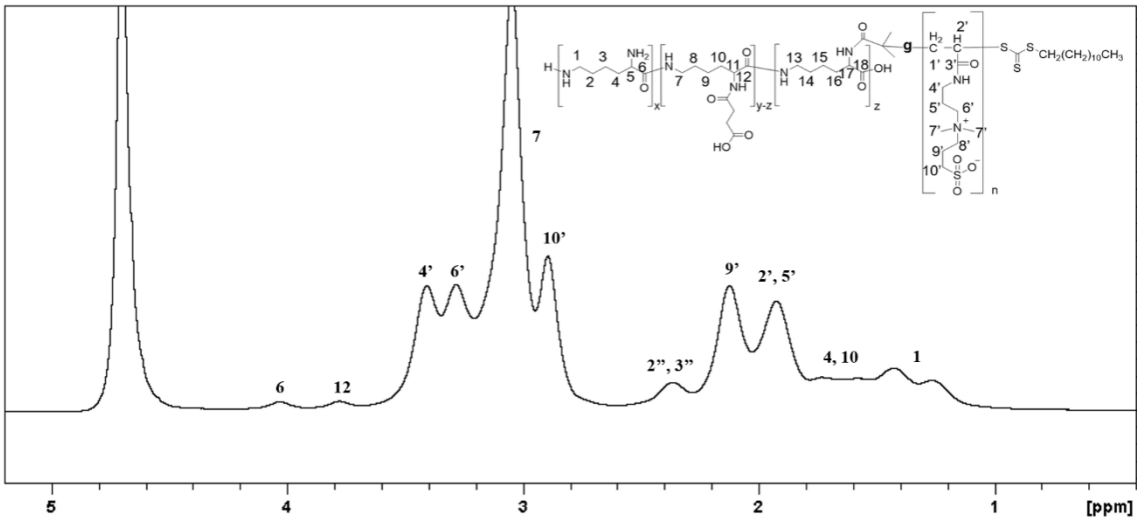

***Figure 2.5**[1]H NMR of P2in D_2O.*

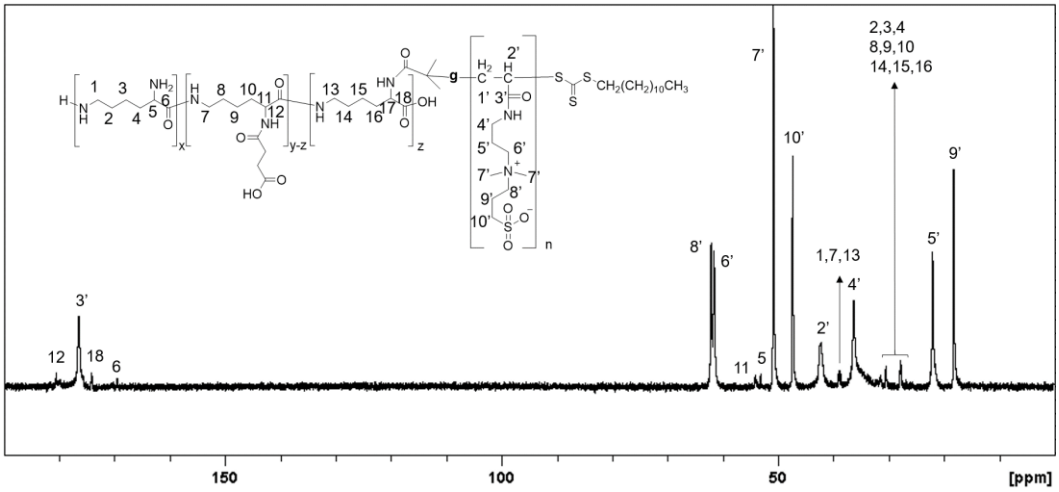

***Figure 2.6**[13]C NMR of P2 in D_2O.*

Table 2.1 *Characteristics of the macro-chain transfer agent (CTA).*

Polymer		DS[b]		Number of NH_2[c]	Number of RAFT agents substituted per chain[e]	
		TNBS[c]	NMR[d]		TNBS[c]	NMR[d]
PLLSA50	In feed	50%		16.73	-	-
	In polymer[a]	46.5%	47%			
PLLSA50 RAFT Agent	In feed	-		15.68	1.05	0.95
	In polymer[a]					
PLLSA65	In feed	65%		10.72	-	-
	In polymer[a]	65.7%	63.6%			
PLLSA65 -RAFT Agent	In feed	-		9.52	1.20	1.25
	In polymer[a]					

Note: [a] Determined by ^1H NMR. [b]Degree of substitution (DS) of SA into PLL. [c]Calculated by the TNBS assay (PLL has ~31 repeating units). [d]Determined by ^1H NMR. [e]Determined by subtracting the number of NH_2 in PLLSA from the RAFT agent substituted PLLSA.

Table 2.2 *Characteristics of graft copolymers prepared via RAFT polymerization.*

Entry	Polymer[a]	Number of repeating units			Molar ratio[c]	$M_n \times 10^{-3}$[b]
			PLLSA	PSPB		
P1	PLLSA(50)-g-PSPB200	In feed	31.25	200	1000:1:5	41.1
		In polymer[b]	31.25	125.4		
P2	PLLSA(65)-g-PSPB200	In feed	31.25	200		58.0
		In	31.25	181.5		

		polymer[b]				

Note: [a]Number in parenthesis next to PLLSA indicates the % substitution of SA in PLL and the subscript next to PSPB denotes the degree of polymerization of SPB.[b]Determined by ^{1}H NMR.[c][Monomer]:[Initiator]:[RAFT agent] (monomer: SPB, initiator: V-501, RAFT agent: PLLSA-RAFT agent).

Time-dependent ^{1}H NMR was used to determine the conversion of SPB in the RAFT polymerization and to study the kinetics of RAFT polymerization. Completion of the reaction was monitored by observing the loss of vinyl protons from the monomer (Figure 2.7 and Figure 2.8). The relationship between $\ln([M]_o/[M])$ and time is shown in Figure 2.9. An almost linear first-order kinetic plot was obtained, suggesting that the reaction follows living polymerization kinetics. After 3 h, the reaction was nearly 70% complete.

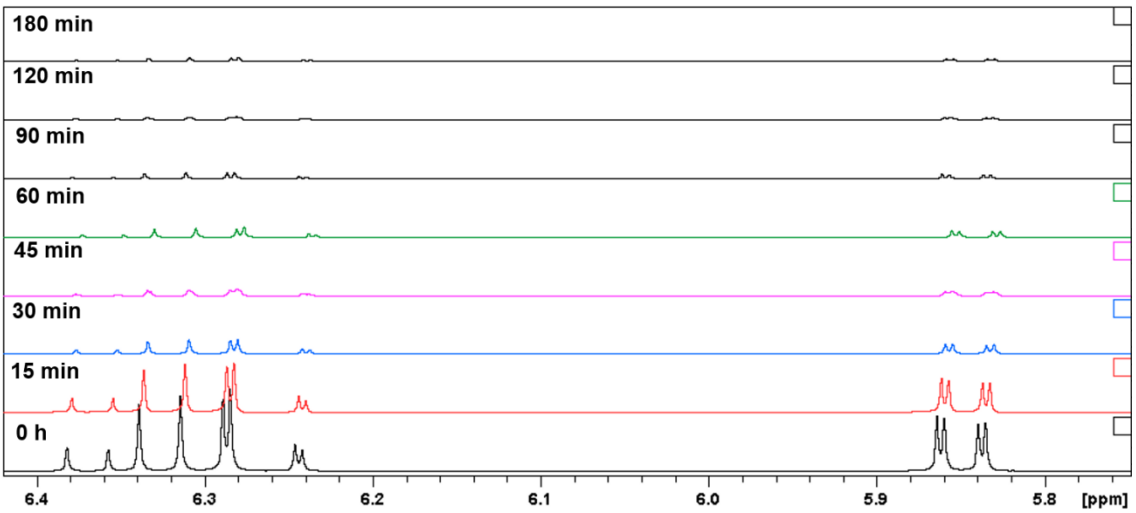

Figure 2.7*Time-dependent ^{1}H-NMR spectra of P1 in D_2O.*

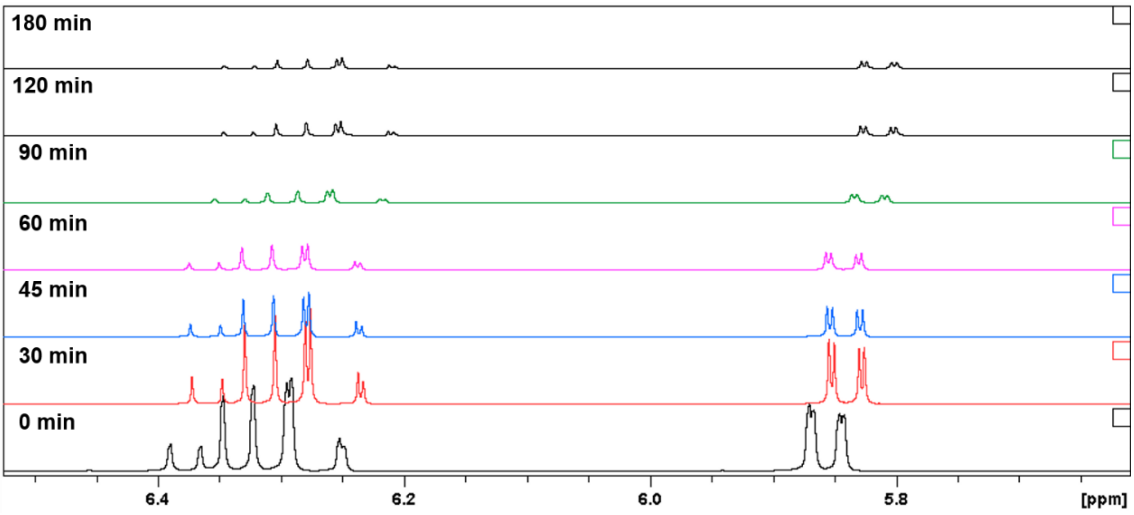

Figure 2.8*Time-dependent ^{1}H-NMR spectra of P2 in D_2O.*

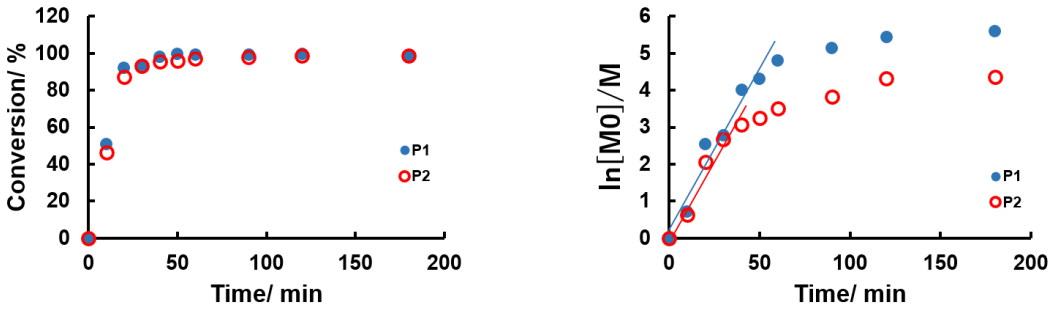

Figure 2.9 *Kinetic plot showing the polymerization of the block copolymer.*

2.3.2 Dual-thermoresponsive Property

Figure 2.10 shows photographs of an aqueous solution containing 1 wt. % of P2 taken at different temperatures. The solution was transparent at 40 °C, while it was turbid at 4 °C and 70 °C. The pictures clearly show that heating and cooling lead to changes in

the solubility of the polymer. This result clearly indicates that this graft copolymer exhibits LCST- and UCST-type phase separation properties.

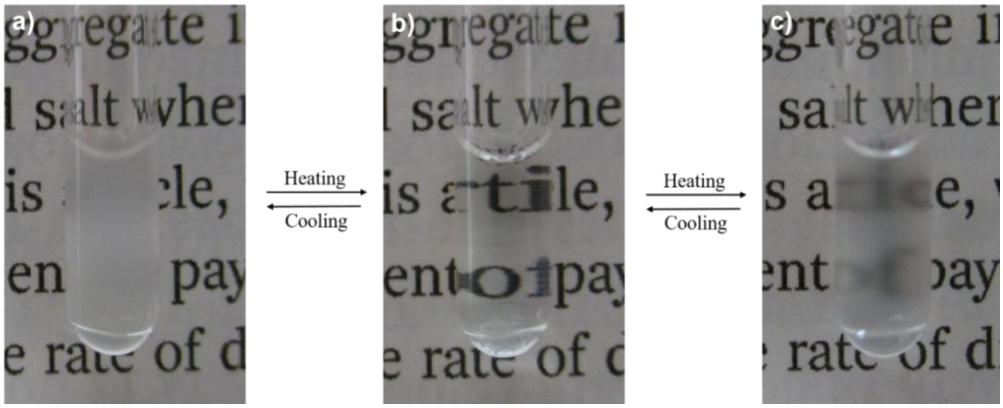

Figure 2.10 *Photographs of the graft copolymer (P2, 1% w/w) before and after cooling. The photographs (a), (b), and (c) were taken at 4 °C, 40 °C, and 70 °C, respectively.*

The thermoresponsive property of the graft copolymers was determined by turbidimetry in water by UV-vis spectroscopy at a 550 nm wavelength. Figure 2.11 shows the phase transition behavior of P1 and P2 at different concentrations. Each of the graft copolymers display both LCST- and UCST-type phase separation behavior. With an increase in temperature, the polymer solution undergoes insoluble-soluble-insoluble transition. Upon heating, the transmittance of the solution increases and as the temperature is further increased, the transmittance of the solution starts decreasing. At low temperatures, the graft copolymer (SPB segment) exhibits UCST-type transition, and at high temperatures, the graft copolymer (PLLSA segment)

exhibits LCST-type transition. For P1 (Figure 2.11a), at 14 °C, the polymer solution is turbid, and the transmittance increases with the temperature. When the temperature reaches 40 °C, the transmittance reaches its maximum value. However, as the temperature increases beyond 44 °C, the transmittance starts decreasing. From around 46 °C to 80 °C, the polymer exhibits LCST behavior (PLLSA segment). The transmittance decreases with further increases in temperature because of the gradual dehydration of the PLLSA chain (LCST transition). Similarly, in the case of P2 (Figure 2.11b), the transmittance of the solution increases when the temperature increases from 16 °C to 46 °C. This is followed by a decrease in transmittance with further increases in the temperature, up to 80 °C. Figure 2.11 clearly shows that the polymer exhibits both a UCST and a LCST behavior. In addition, we observe that the slope of the curve corresponding to a UCST behavior is larger than that corresponding to a LCST behavior; this is because the graft copolymer contains more UCST segments than LCST segments, i.e., more repeating units of PSPB are present as compared to those of PLLSA (Table 2.2). Meanwhile, the electrostatic interaction between the PSPB chain and PLLSA chain might affect the speed with which the transmittance decreases.

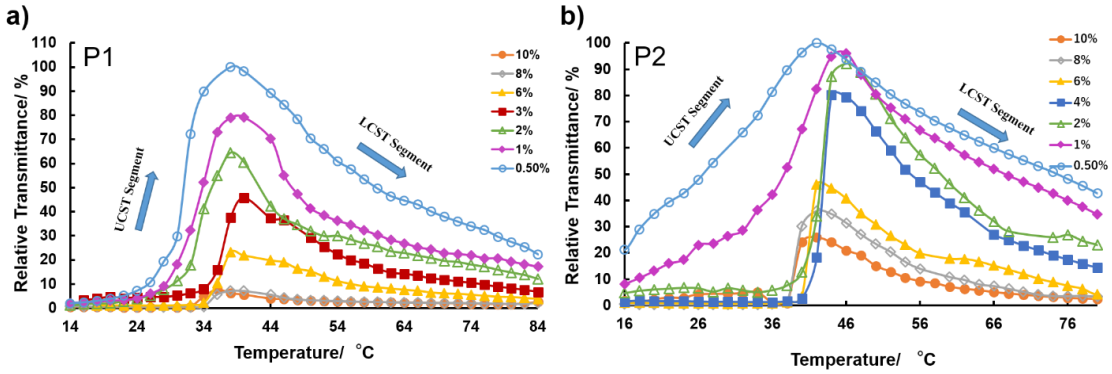

Figure 2.11*Relative transmittance of polymer solutions of (a) P1 and (b) P2 at various concentrations.*

The phase diagram for the graft copolymers was plotted by gathering the points at which the transmittance reaches half of its maximum value. From Figure 2.12, we can see that the phase separation temperature was affected by both the degree of polymerization of the SPB and the degree of the substitution of SA in PLL. The cloud points of P1 were slightly higher than that of P2 because in P2, the degree of polymerization of the SPB was higher than that of P1. This result is consistent with the results shown in Figure 2.11. The UCST increases because an increase in M_n leads to a decrease in the mixing entropy.[49] The LCST of P2 is higher than that of P1; this result is also consistent with those of previous studies.[24] Because PLLSA50 contains an equal number of amino and carboxyl groups, the interactions between the two groups is stronger than that of PLLSA65; hence, P1 shows phase separation at lower temperatures. Figure 2.12a and Figure 2.12b show the phase diagrams of the PSPB and PLLSA

homopolymers. For the PSPB homopolymer, the cloud points of the PSPB homopolymer increased with increasing concentration, indicating a similar trend observed in Figure 2.13. Figure 2.12bshows the phase diagrams of the PLLSA50 homopolymer. Compared to the graft polymer, we found that, after grafting PSPB on the PLLSA, the cloud points of the PSPB and PLLSA are higher than those of the homopolymers. The increase in cloud points is possible due to the PLLSA segment acting as a hydrophilic segment at the temperature lower than the LCST and the PSPB segment acting as a hydrophilic segment at the temperature above the UCST. This corresponds well with the understanding that the addition of a hydrophilic segment increases the phase transition temperature.[24]Figure 2.12c shows the hysteresis curves of P1 at 2% concentration. These curves were achieved by measuring the transmittance on first increasing the temperature gradually until 70 °C followed by cooling. Very small hysteresis on heating and cooling cycles was observed from the curves.

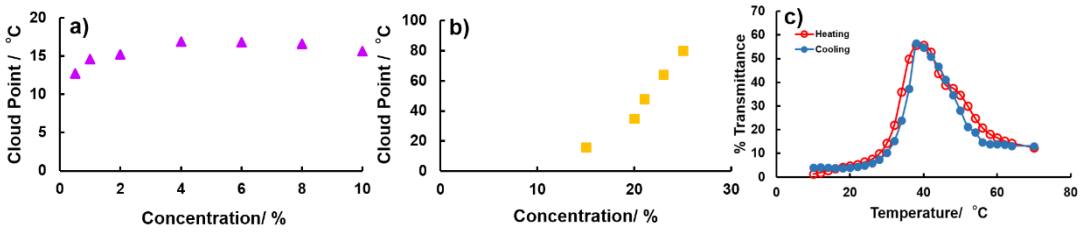

Figure 2.12. *Phase diagrams of a) PSPB homopolymer solution and b) PLLSA50 polymer solution. c) Hysteresis curves of 2% (w/w) P1 in distilled water. Red line: heating; blue line: cooling.*

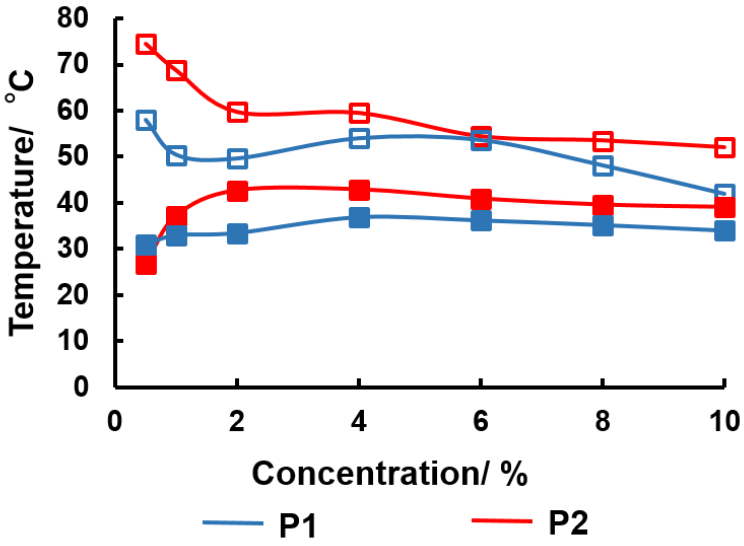

***Figure 2.13**.Phase diagram of the polymer solutions of P1 and P2; the open squares represent LCST transitions and the closed squares represent UCST transitions.*

The size of these graft copolymers was then studied using DLS 0.75% (w/w). As shown in Figure 2.14, at lower and higher temperatures, the size of the polymers aggregates was larger than those at medium temperatures (around 30–40 °C), indicating that at lower and higher temperatures, the SPB segment and PLLSA segments aggregated. This result also corresponds well with the result obtained by UV-Vis spectroscopy. Moreover, the PLLSA segments aggregate at higher temperatures, which is why the polymer shows larger size aggregates. The size of the polymer aggregates at high temperature is larger than that at low temperature.

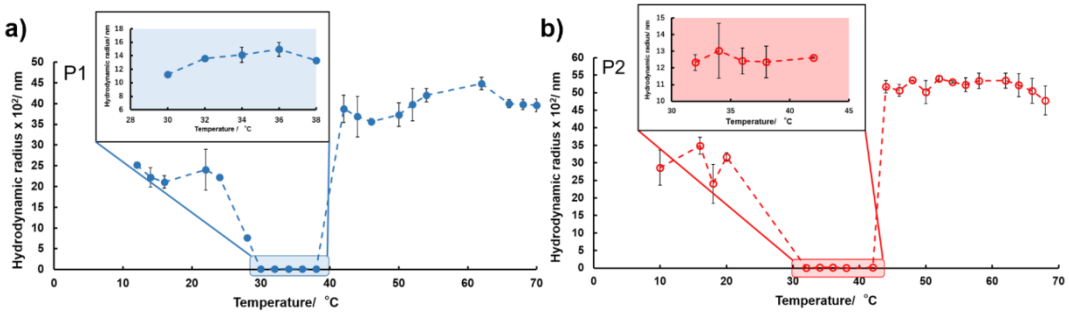

Figure 2.14.*Temperature-dependent DLS measurements of the graft copolymer in water at a polymer concentration of 0.75 % for a) P1 and b) P2.*

2.3.3 pH-responsive Property

The pH-responsive property was investigated by UV-Vis spectroscopy by measuring the change in transmittance with the change of pH. Figure 2.15 shows that the transmittance increased with an increase or decrease in the pH of the solution. At pH 1 and pH 13, the transmittance achieved its maximum value. Following pH change, more H^+ or OH^- were added into the solution, which affected the hydrogen bonds or the electrostatic interaction in PLLSA and in SPB, resulting in the solution changing from turbid to transparent.

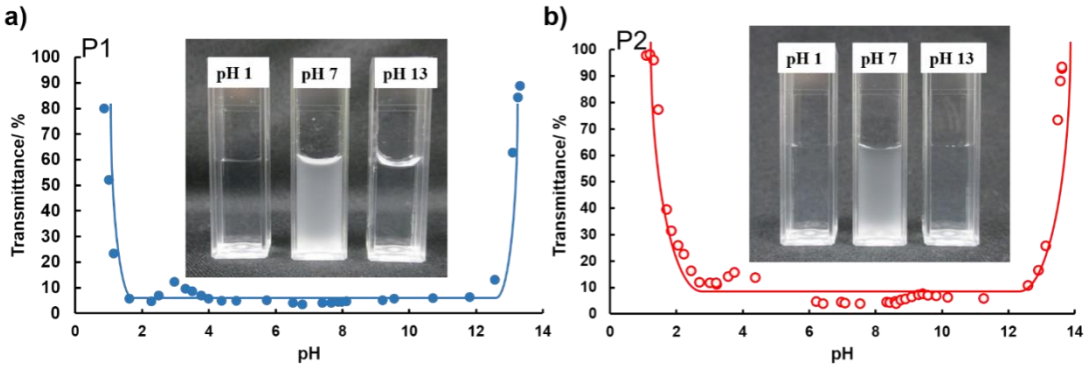

Figure 2.15.*Relative transmittance of polymer solutions of (a) P1 (1% w/w) and (b) P2 (1% w/w) at various pH values at 25° C.*

Figure 2.16 shows the zeta potential results of the graft copolymers at different pH values. Because P2 contains negatively charged PLLSA (65), the zeta potential is more negative than that of P1. Moreover, at ~pH 7, both P1 and P2 exhibit negative charges, and with a decrease in the pH, the zeta potential of these polymers becomes positive. This interesting property can be potentially used to deliver any positively charged protein or drug, and we exploited this property to release a positively charged protein in this study. The isoelectric point calculated by the pH at which zeta potential becomes neutral is 5.5 for P1 and 4.6 for P2.

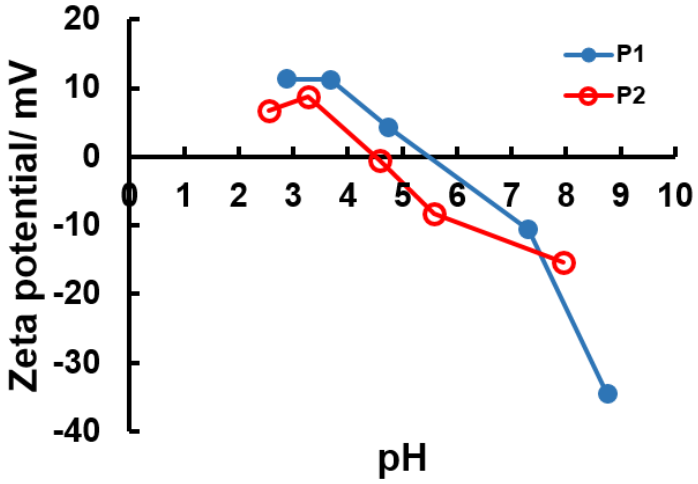

Figure 2.16 *Measurement of the zeta potentials of the polymer solutions of P1 (1% w/w) and P2 (1% w/w) at different pH values.*

2.3.4 Protein release

A positively charged protein can be bound to a negatively charged polymer via electrostatic interaction. As can be seen from the results above, when the pH value of the polymers was 3, the charge of the polymers changed from negative to positive; therefore, if a positively charged protein is bound to such a polymer at the physiological pH, the protein can be released owing to electrostatic repulsion when lowering the pH. Lysozyme was chosen as the model protein for this study. This is primarily because of the net positive charge of this protein.[50] Moreover, its structural details have been studied extensively, and complete information about its higher order structures is

known.[51, 52]Forthis study, the polymer and lysozyme were dissolved in PBS (pH 7.4) and then incubated at 25 °C for 1 h. The solution was then transferred to the centrifugal filter units with MWCO 30K and then centrifuged at 15 °C at 13.2 × 1000 rpm for 2 h. The solution at the bottom consisted of unbound lysozyme and the filter at the top retained the protein bound to the polymer. The amount of unbound protein was quantified by a Bradford assay using the Bradford Ultra reagent (Expedeon Ltd., Harston, UK). By using equation (1), it was found that 94.25% of the protein was successfully bound to the polymer.

The protein release experiment was performed using DLS. The solution containing polymer-bound protein, which stayed on top, was collected, and the pH was changed to 3. DLS was employed to measure the hydrodynamic radius of the polymer and that of the protein before and after pH change. From Figure 2.17, we clearly see that a peak appeared around 1000 nm (blue line with open circles) after changing the pH to 3. Before changing the pH of the solution (pH 7.4), only one peak (yellow line with closed circles) was present, which indicated that the protein was completely bound with the polymer. However, the protein released showed slight aggregation, which may be due to the duration of the centrifugation.

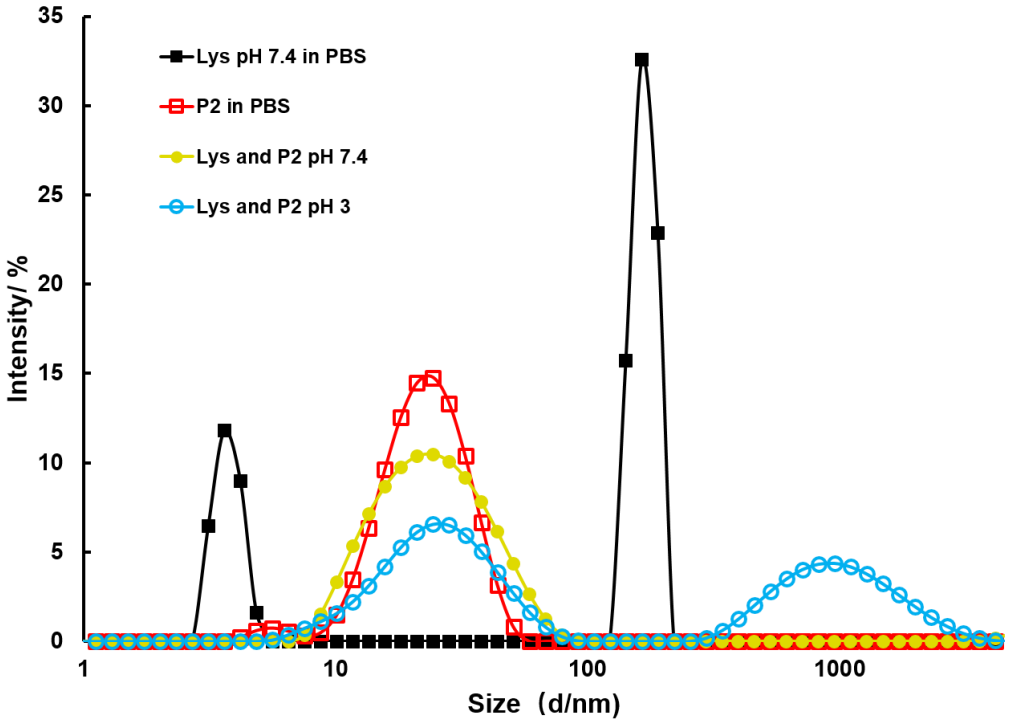

Figure 2.17.*Particle size of the lysozyme polymer solution at different pH.*

2.3.5 Protein aggregation inhibition

Figure 2.18 shows photographs taken after lysozyme treatment at 90 °C for 30 min with and without the polymer. The native lysozyme solution was obtained by dissolving lysozyme in PBS (pH 7.4, 1 mg/mL) (Figure 2.18a). A clear aggregation can be seen in Figure 2.18b; this photograph was taken after the lysozyme solution was heated at 90 °C for 30 min without the addition of any polymer. In contrast, when the lysozyme solution was heated at 90 °C for 30 min in the presence of 5% (w/v) P1 (Figure 2.18c) or P2 (Figure 2.18d), no significant aggregation could be seen. These results clearly show that

P1 and P2 possess lysozyme aggregation inhibition properties. To quantify the extent of aggregation and protection, and to investigate any changes in the higher-order structure of proteins on aggregation, further studies were conducted.

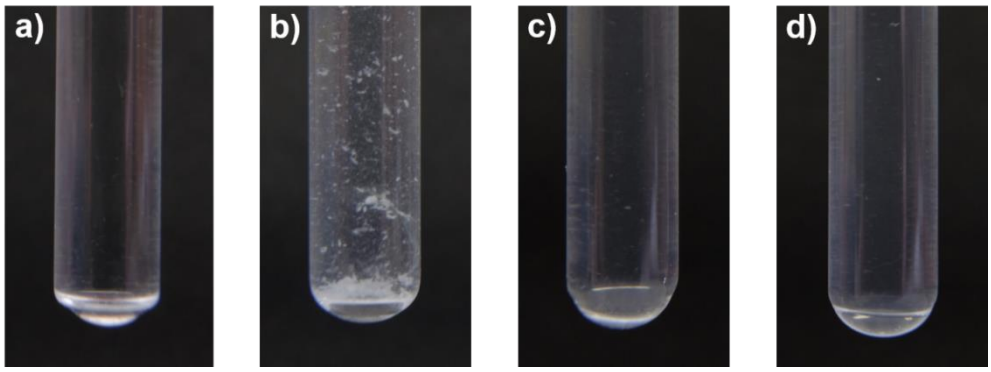

Figure 2.18.*Photographs of lysozyme in PBS (1 mg/mL): a) native lysozyme; b) treatment at 90° C for 30 min without polymer presence; c) with 5% (w/w) of P1; and d) with 5% (w/w) of P2.*

2.3.6 Amyloid Fibril Formation

Figure 2.19ashows the result of the fibril formation of lysozyme in the presence of different concentrations of the polymer after heating for 30 min at 90 °C. The ThT assay was used to determine the amount of the amyloid fibrils in solution. We found that when the polymer concentration increased, the intensity of ThT fluorescence started decreasing. This clearly indicates that addition of the graft copolymer suppresses the formation of fibrils. The ThT fluorescence observed was less than 10% when 5% of P2 was present. In comparison with P1, P2 showed higher efficiency in suppressing the formation of amyloid fibrils. In this study, as P2 exhibits an overall negative charge,

which enables a stronger interaction with the positively charged lysozyme, the formation of fibrils is suppressed to a greater extent than that by P1. Furthermore, it has been established that hydrophobic interaction plays an important role in protein fibril formation and also that ampholytic polymers act as molecular shields that reduce the formation of the fibrils.[34] Another possible explanation for the increased efficiency of P2 against fibril formation is the prevention of interactions between the hydrophobic domains of the protein owing to their electrostatic interactions with the polymer.

2.3.7 Residual Enzymatic Activity

To assess the proficiency of the graft copolymers in protecting proteins after heat treatment, we investigated the residual enzymatic activity of lysozyme. The enzymatic activity of lysozyme after heat treatment was investigated by the decrease in turbidity of a Micrococcus lysodeikticus cell suspension following the addition of lysozyme. Faster breakdown of the Micrococcus lysodeikticus cell suspension represents higher residual activity of lysozyme, indicated by a decrease in the turbidity of the solution, which was monitored by UV-Vis spectroscopy. From Figure 2.19b, we can clearly see that the activity of lysozyme is maintained in the presence of both P1 and P2. Nearly 70% of lysozyme remains active in the presence of a 5% concentration of P2. Compared with

our previous work, these polymers exhibit more efficiency in protecting lysozyme than that of linear poly-SPB.[34, 53]The lysozyme protective property of P2 is higher than that of P1. This is in agreement with the results obtained with ThT, which revealed that the negatively charged P2 interacted more strongly with lysozyme, leading to increased protection. Complete loss in activity was calculated by heating lysozyme solution without any additive and the percent residual activity was calculated relative to these values.

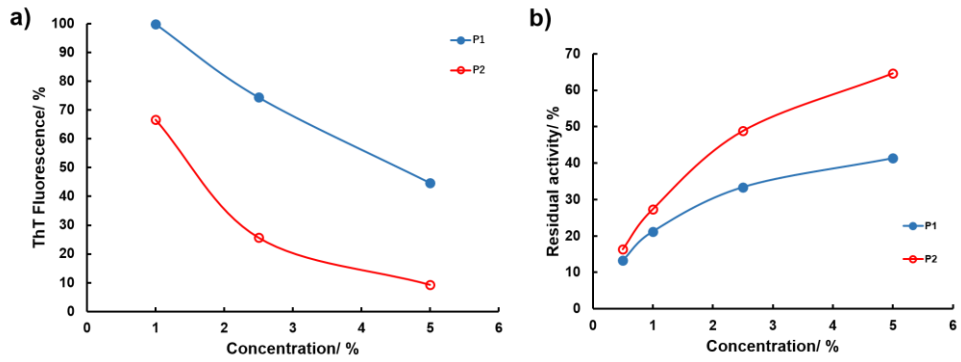

Figure 2.19. *a)Analysis of fibril formation of lysozyme in the presence of different concentrations of polymers after treatment at 90 °C for 30 min as determined by the ThT fluorescence assay. b) Residual activity of lysozyme in the presence of different concentrations of polymers after treatment at 90 °C for 30 min. The activity was measured with a UV-Vis spectrophotometer.*

2.3.8 CD Spectroscopy

The change in the secondary structure of the lysozyme was analyzed by CD spectroscopy. All collected data were the average of three scans and were measured in

the presence of N_2 gas. As shown in Figure 2.20a, the CD spectra of native lysozyme without heating showed negative peaks near 205 nm and 220 nm, indicating the presence of the β-sheet and α–helix structure.[54] After heating for 30 min at 90 °C, the intensity of these peaks decreased significantly, indicating that high temperature leads to the loss of the α– helix and β-sheet structure (red line). However, after addition of the polymer (5% w/w), the negative peaks near 205 nm and 220 nm were retained with almost the same intensity as that observed with native lysozyme. This indicates that these graft copolymers help in the retention of the secondary structure of lysozyme. Further, to confirm the ratio of each secondary structure element, the CDSSTR algorithm with the reference set 7 of the DichroWeb server was used to deconvolute the CD spectra.[55, 56] We observed the following secondary structure contents, as shown in Figure 2.10b: lysozyme without heating: 45% α– helix, 21% strand, 14% turn, and 21% unordered; lysozyme with heating: 5% α– helix, 28% stand, 18% turn, and 48% unordered. Considerable decrease in the α– helix content was seen after high temperature treatment, and this was compensated for by an increase in the amount of the unordered conformation. A slight increase in the β-strand was also observed. This clearly indicates that high-temperature treatment completely alters the higher structure of lysozyme. It is worth noting that, in the presence of 5% (w/w) P1 and P2, the fraction

of the secondary structure elements did not show significant change compared with lysozyme without heating. Although a slight decrease in the α-helix portion was observed, almost all of the secondary structure of the lysozyme was retained in the presence of these graft copolymers. The ability of P2 to retain the secondary structure was slightly higher than that of P1, and this is consistent with the results obtained from the ThT assay and residual enzymatic activity. The retention of the higher-order structure of lysozyme in the presence of these graft copolymers stabilizes lysozyme and enables solubility in the buffer even after high temperature treatment, thus suppressing the aggregation of lysozyme.

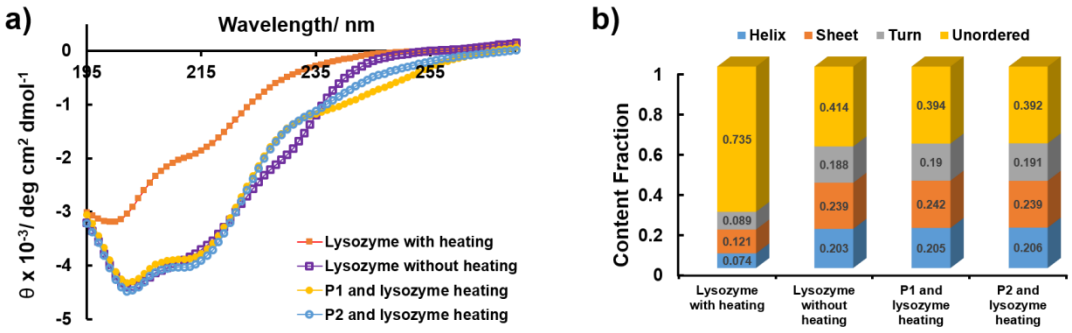

Figure 2.20. *a)Representative far-UV CD spectra of lysozyme in the absence and presence of polymers (5% w/w) after incubation at 90 °C for 30 min. b) The contents of the secondary structure of lysozyme.*

2.3.9 Cytotoxicity Assay

Figure 2.21 shows the cytotoxicity of the polymers, and the results clearly demonstrate that both P1 and P2 show very low toxicity, even at very high concentrations of the polymer (5% w/w), with cell viability observed to be greater than 60%. Usually, cytotoxicity is evaluated by the concentration of the test compound needed to kill half of the cells, IC_{50}. IC_{50} was not observed at these concentrations. Low toxicity indicates these polymers are extremely biocompatible and can be safely used in living organisms for various biomedical applications.

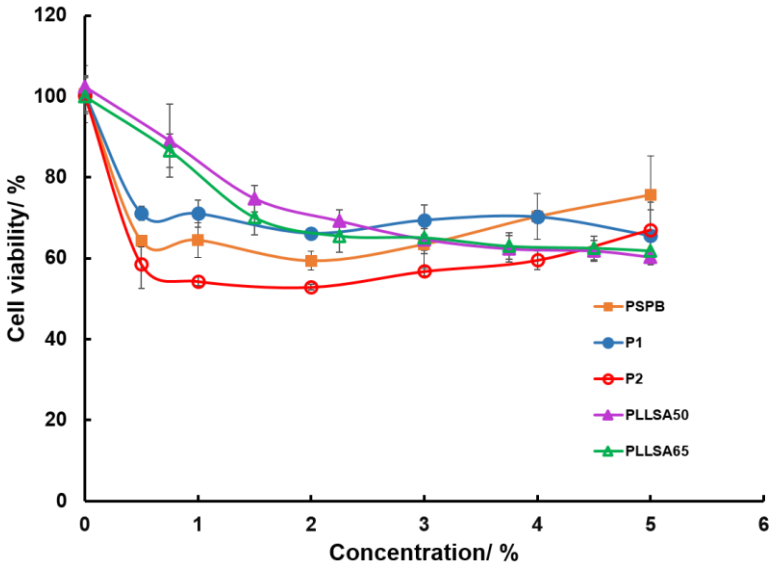

Figure 2.21. *Cytotoxicity of the polymers. L929 cells were treated with different concentrations of polymers: PSPB (closed squares), P1 (closed circles), P2 (open circles), PLLSA50 (closed triangles), and PLLSA65 (open triangles).*

2.4 Conclusion

In conclusion, two dual-thermo- and pH-responsive graft copolymers were successfully synthesized by RAFT polymerization. These graft copolymers contain two different polyampholyte segments. To the best of the authors' knowledge, this is the first study to use PLLSA as an LCST-inducing segment in a graft copolymer, thus imparting a new and interesting characteristic to the graft copolymer. The presence of two zwitterionic segments not only allows the graft copolymer to exhibit a dual-temperature responsive property, but also allows the polymer to exhibit a pH-responsive property. Interestingly, we found these polymers can have multiple functionalities, i.e., they can be used as a protein release vehicle and, at the same time, can suppress protein aggregation under severe stress. A very high protein protection efficiency was observed, with more than 70% of the activity being retained even after heating at very high temperatures, and the secondary structure of the lysozyme was also retained in the presence of these graft copolymers. Unlike in other systems that contain non-ionic segments, the critical solution temperature of the polymers in the proposed system, which contains two polyampholyte segments, can be changed by changing the various parameters of the graft copolymers. Moreover, the easy tunability can potentially allow these graft copolymers to be used in a variety of applications, such as

in sensitivity-tunable sensors or in the design of thermo optical devices. Further, these polymers can be easily transformed into multi-stimuli-responsive self-assembled nanogels, micelles, or other types of vesicles to enable controlled release of proteins. Additionally, the ability to load and release proteins by changing the environmental conditions and enabling protection under severe stress can allow them to be used for the prevention or treatment of many neurodegenerative diseases. A direct extension of this study would be to study the controlled release of other biologically relevant proteins as protein drugs or as antimicrobial peptides. Research on utilizing the dual-thermo responsive property of such polymers for the release of drugs and proteins by changing the polymer architecture and composition is underway.

2.5 References

(1) Ariga, K.; Kawakami, K.; Ebara, M.; Kotsuchibashi, Y.; Ji, Q.; Hill, J. P. Bioinspired Nanoarchitectonics as Emerging Drug Delivery Systems. *New J. Chem.***2014**, *38* (11), 5149–5163.

(2) Aghabegi Moghanjoughi, A.; Khoshnevis, D.; Zarrabi, A. A Concise Review on Smart Polymers for Controlled Drug Release. *Drug Deliv. Transl. Res.***2016**, *6* (3), 333–340.

(3) Jung, Y. seok; Park, W.; Park, H.; Lee, D. K.; Na, K. Thermo-Sensitive Injectable Hydrogel Based on the Physical Mixing of Hyaluronic Acid and Pluronic F-127 for Sustained NSAID Delivery. *Carbohydr. Polym.***2017**, *156*, 403–408.

(4) Wang, G.; Nie, Q.; Zang, C.; Zhang, B.; Zhu, Q.; Luo, G.; Wang, S. Self-Assembled Thermoresponsive Nanogels Prepared by Reverse Micelle → Positive Micelle Method for Ophthalmic Delivery of Muscone, a Poorly Water-Soluble Drug. *J. Pharm. Sci.***2016**, *105* (9), 2752–2759.

(5) Madhusudana Rao, K.; Mallikarjuna, B.; Krishna Rao, K. S. V.; Siraj, S.; Chowdoji Rao, K.; Subha, M. C. S. Novel Thermo/PH Sensitive Nanogels Composed from Poly(N-Vinylcaprolactam) for Controlled Release of an Anticancer Drug. *Colloids Surfaces B Biointerfaces***2013**, *102*, 891–897.

(6) Shen, Y.; Li, G.; Ma, Y.; Yu, D.; Sun, J.; Li, Z. Smart Surfaces Based on Thermo-Responsive Polymer Brushes Prepared from l-Alanine Derivatives for Cell Capture and Release. *Soft Matter***2015**, *11* (38), 7502–7506.

(7) Ebara, M.; Akimoto, M.; Uto, K.; Shiba, K.; Yoshikawa, G.; Aoyagi, T. Focus on the Interlude between Topographic Transition and Cell Response on Shape-Memory Surfaces. *Polymer (Guildf).***2014**, *55* (23), 5961–5968.

(8) Mosqueira, D.; Pagliari, S.; Uto, K.; Ebara, M.; Romanazzo, S.; Escobedo-Lucea, C.; Nakanishi, J.; Taniguchi, A.; Franzese, O.; Di Nardo, P.; Goumans, M. J.; Traversa, E.; Pinto-do-Ó, P.; Aoyagi, T.; Forte, G. Hippo Pathway Effectors Control Cardiac Progenitor Cell Fate by Acting as Dynamic Sensors of Substrate Mechanics and Nanostructure. *ACS Nano***2014**, *8* (3), 2033–2047.

(9) Kim, Y. J.; Kim, S. H.; Fujii, T.; Matsunaga, Y. T. Dual Stimuli-Responsive Smart Beads That Allow "on-off" Manipulation of Cancer Cells. *Biomater. Sci.***2016**, *4* (6), 953–957.

(10) Paulus, A. S.; Heinzler, R.; Ooi, H. W.; Franzreb, M. Temperature-Switchable Agglomeration of Magnetic Particles Designed for Continuous Separation Processes in Biotechnology. *ACS Appl. Mater. Interfaces***2015**, *7* (26), 14279–14287.

(11) Yoshimatsu, K.; Lesel, B. K.; Yonamine, Y.; Beierle, J. M.; Hoshino, Y.; Shea, K. J. Temperature-Responsive "Catch and Release" of Proteins by Using

Multifunctional Polymer-Based Nanoparticles. *Angew. Chemie - Int. Ed.***2012**, *51* (10), 2405–2408.

(12) Klaikherd, A.; Nagamani, C.; Thayumanavan, S. Multi-Stimuli Sensitive Amphilic Block Copolymer Assemblies. *J. Am. Chem. Soc.***2009**, *131* (13), 4830–4838.

(13) Song, Z.; Wang, K.; Gao, C.; Wang, S.; Zhang, W. A New Thermo-, PH-, and CO 2 -Responsive Homopolymer of Poly[N-[2-(Diethylamino)Ethyl]Acrylamide]: Is the Diethylamino Group Underestimated? *Macromolecules***2016**, *49* (1), 162–171.

(14) Ganesh, V. A.; Baji, A.; Ramakrishna, S. Smart Functional Polymers - A New Route towards Creating a Sustainable Environment. *RSC Adv.***2014**, *4* (95), 53352–53364.

(15) Fournier, D.; Hoogenboom, R.; Thijs, H. M. L.; Paulus, R. M.; Schubert, U. S. Tunable PH- and Temperature-Sensitive Copolymer Libraries by Reversible Addition-Fragmentation Chain Transfer Copolymerizations of Methacrylates. *Macromolecules***2007**, *40* (4), 915–920.

(16) Guragain, S.; Bastakoti, B. P.; Malgras, V.; Nakashima, K.; Yamauchi, Y. Multi-Stimuli-Responsive Polymeric Materials. *Chem. - A Eur. J.***2015**, *21* (38), 13164–13174.

(17) Rajan, R.; Matsumura, K. Tunable Dual-Thermoresponsive Core–Shell Nanogels Exhibiting UCST and LCST Behavior. *Macromol. Rapid Commun.***2017**, *38* (22) 1700478.

(18) Vishnevetskaya, N. S.; Hildebrand, V.; Niebuur, B.; Grillo, I.; Filippov, S. K.; Laschewsky, A.; Mu, P.; Papadakis, C. M. Aggregation Behavior of Doubly Thermoresponsive Polysulfobetaine - b - Poly(N - Isopropylacrylamide) Diblock Copolymers. *Macromolecules*, **2016,**49, 6655–6668.

(19) Vishnevetskaya, N. S.; Hildebrand, V.; Dyakonova, M. A.; Niebuur, B.; Kyriakos, K.; Raftopoulos, K. N.; Di, Z.; Mu, P.; Laschewsky, A.; Papadakis, C. M. Dual Orthogonal Switching of the " Schizophrenic " Self-Assembly of Diblock Copolymers. *Macromolecules*, **2018**, 51, 2604–2614.

(20) Vishnevetskaya, N. S.; Hildebrand, V.; Niebuur, B.; Grillo, I.; Filippov, S. K.; Laschewsky, A.; Mu, P.; Papadakis, C. M. " Schizophrenic " Micelles from Doubly

Thermoresponsive Polysulfobetaine - b - Poly(N - Isopropylmethacrylamide) Diblock Copolymers. *Macromolecules*, **2017**, 50, 3985–3999.

(21) Bromberg, L.; Levin, G. Poly(Amino Acid)-b-Poly(N,N-Diethylacrylamide)-b-Poly(Amino Acid) Conjugates of Well-Defined Structure. *Bioconjug. Chem.***1998**, *9* (1), 40–49.

(22) Kim, S. W.; Jeong, B.; Bae, Y. H.; Lee, D. S. Biodegradable Block Copolymers as Injectable Drug-Delivery Systems. *Nature***1997**, *388* (6645), 860–862.

(23) Furyk, S.; Zhang, Y.; Ortiz-Acosta, D.; Cremer, P. S.; Bergbreiter, D. E. Effects of End Group Polarity and Molecular Weight on the Lower Critical Solution Temperature of Poly(*N*-Isopropylacrylamide). *J. Polym. Sci. Part A Polym. Chem.***2006**, *44* (4), 1492–1501.

(24) Das, E.; Matsumura, K. Tunable Phase-Separation Behavior of Thermoresponsive Polyampholytes through Molecular Design. *J. Polym. Sci. Part A Polym. Chem.***2017**, *55* (5), 876–884.

(25) Wang, Y. W.; Chen, L. Y.; An, F. P.; Chang, M. Q.; Song, H. B. A Novel Polysaccharide Gel Bead Enabled Oral Enzyme Delivery with Sustained Release in Small Intestine. *Food Hydrocoll.***2018**, *84* (November 2017), 68–74.

(26) Shih, I. L.; Shen, M. H.; Van, Y. T. Microbial Synthesis of Poly(ε-Lysine) and Its Various Applications. *Bioresour. Technol.***2006**, *97* (9), 1148–1159.

(27) Matsumura, K.; Hyon, S. H. Polyampholytes as Low Toxic Efficient Cryoprotective Agents with Antifreeze Protein Properties. *Biomaterials***2009**, *30* (27), 4842–4849.

(28) Zhang, W.; Yang, Z.; Kaufman, Y.; Bernstein, R. Surface and Anti-Fouling Properties of a Polyampholyte Hydrogel Grafted onto a Polyethersulfone Membrane. *J. Colloid Interface Sci.***2018**, *517*, 155–165.

(29) Zhang, W.; Cheng, W.; Ziemann, E.; Be'er, A.; Lu, X.; Elimelech, M.; Bernstein, R. Functionalization of Ultrafiltration Membrane with Polyampholyte Hydrogel and Graphene Oxide to Achieve Dual Antifouling and Antibacterial Properties. *J. Memb. Sci.***2018**, *565* (August), 293–302.

(30) Ahmed, S.; Hayashi, F.; Nagashima, T.; Matsumura, K. Protein Cytoplasmic Delivery Using Polyampholyte Nanoparticles and Freeze Concentration. *Biomaterials***2014**, *35* (24), 6508–6518.

(31) Laschewsky, A. Structures and Synthesis of Zwitterionic Polymers. *Polymers (Basel).***2014**, *6* (5), 1544–1601.

(32) Rajan, R.; Jain, M.; Matsumura, K. Cryoprotective Properties of Completely Synthetic Polyampholytes via Reversible Addition-Fragmentation Chain Transfer (RAFT) Polymerization and the Effects of Hydrophobicity. *J. Biomater. Sci. Polym. Ed.***2013**, *24* (15), 1767–1780.

(33) Lowe, A. B.; Vamvakaki, M.; Wassall, M. A.; Wong, L.; Billingham, N. C.; Armes, S. P.; Lloyd, A. W. Well-Defined Sulfobetaine-Based Statistical Copolymers as Potential Antibioadherent Coatings. *J. Biomed. Mater. Res.***2000**, *52* (1), 88–94.

(34) Rajan, R.; Matsumura, K. A Zwitterionic Polymer as a Novel Inhibitor of Protein Aggregation. *J. Mater. Chem. B***2015**, *3* (28), 5683–5689.

(35) Rajan, R.; Matsumura, K. Inhibition of Protein Aggregation by Shell Nanogels. *Sci. Rep.***2017**, No. March, 1–9.

(36) Rajan, R.; Suzuki, Y.; Matsumura, K. Zwitterionic Polymer Design That Inhibits Aggregation and Facilitates Insulin Refolding : Mechanistic Insights and Importance of Hydrophobicity. *Macromol. Biosci.***2018**, *1800016*, 1–6.

(37) He, N.; Lu, Z.; Zhao, W. PH-Responsive Double Hydrophilic Protein-Polymer Hybrids and Their Self-Assembly in Aqueous Solution. *Colloid Polym. Sci.***2015**, *293* (12), 3517–3526.

(38) Cao, Q.; He, N.; Wang, Y.; Lu, Z. Self-Assembled Nanostructures from Amphiphilic Globular Protein–Polymer Hybrids. *Polym. Bull.***2018**, *75* (6), 2627–2639.

(39) Ge, J.; Neofytou, E.; Lei, J.; Beygui, R. E.; Zare, R. N. Protein-Polymer Hybrid Nanoparticles for Drug Delivery. *Small***2012**, *8* (23), 3573–3578.

(40) Wu, C.; Baldursdottir, S.; Yang, M.; Mu, H. Lipid and PLGA Hybrid Microparticles as Carriers for Protein Delivery. *J. Drug Deliv. Sci. Technol.***2018**, *43*, 65–72.

(41) Liu, Z.; Dong, C.; Wang, X.; Wang, H.; Li, W.; Tan, J.; Chang, J. Self-Assembled Biodegradable Protein-Polymer Vesicle as a Tumor-Targeted Nanocarrier. *ACS Appl. Mater. Interfaces***2014**, *6* (4), 2393–2400.

(42) Matsudo, T.; Ogawa, K.; Kokufuta, E. Complex Formation of Protein with Different Water-Soluble Synthetic Polymers. *Biomacromolecules***2003**, *4* (6), 1794–1799.

(43) Sandanaraj, B. S.; Vutukuri, D. R.; Simard, J. M.; Klaikherd, A.; Hong, R.; Rotello, V. M.; Thayumanavan, S. Noncovalent Modification of Chymotrypsin Surface Using an Amphiphilic Polymer Scaffold: Implications in Modulating Protein Function. *J. Am. Chem. Soc.***2005**, *127* (30), 10693–10698.

(44) Jiang, Y.; Lu, H.; Yee Khine, Y.; Dag, A.; H. Stenzel, M. Polyion Complex Micelle Based on Albumin–Polymer Conjugates: Multifunctional Oligonucleotide Transfection Vectors for Anticancer Chemotherapeutics. *Biomacromolecules***2014**, *15* (11), 4195–4205.

(45) Kao, C. H.; Wang, J. Y.; Chuang, K. H.; Chuang, C. H.; Cheng, T. C.; Hsieh, Y. C.; Tseng, Y. long; Chen, B. M.; Roffler, S. R.; Cheng, T. L. One-Step Mixing with Humanized Anti-MPEG Bispecific Antibody Enhances Tumor Accumulation and Therapeutic Efficacy of MPEGylated Nanoparticles. *Biomaterials***2014**, *35* (37), 9930–9940.

(46) Habeeb, A. F. S. A. Determination of Free Amino Groups in Proteins by Trinitrobenzenesulfonic Acid. *Anal. Biochem.***1966**, *14* (3), 328–336.

(47) Ismail, A. M. A Rapid and Sensitive Method for the Quantitation of Microgram Quantities of Protein Utilizing the Principle of Protein-Dye Binding. *Anal. Biochem.***1976**, *72* (1–2), 248–254.

(48) Taneja, S.; Ahmad, F. Increased Thermal Stability of Proteins in the Presence of Amino Acids. *Biochem. J.***1994**, *303*, 147–153.

(49) Seuring, J.; Agarwal, S. Polymers with Upper Critical Solution Temperature in Aqueous Solution. *Macromol. Rapid Commun.***2012**, *33*, 1898–1920.

(50) Ghaderi, R.; Carlfors, J. Biological Activity of Lysozyme After Entrapment in Poly (d,l-Lactide-Co-Glycolide)-Microspheres. *Pharm. Res.***1997**, *14* (11), 1556–1562.

(51) CANFIELD, R. E. The Amino Acid Sequence of Egg White Lysozyme. *J. Biol. Chem.***1963**, *238* (8), 2698–2707.

(52) BLAKE, C. C. F.; KOENIG, D. F.; MAIR, G. A.; NORTH, A. C. T.; PHILLIPS, D. C.; SARMA, V. R. Structure of Hen Egg-White Lysozyme: A

Three-Dimensional Fourier Synthesis at 2 Å Resolution. *Nature***1965**, *206* (4986), 757–761.

(53) Sharma, N.; Rajan, R.; Makhaik, S.; Matsumura, K. Comparative Study of Protein Aggregation Arrest by Zwitterionic Polysulfobetaines : Using Contrasting Raft Agents. *ACS Omega***2019**, *4*, 12186–12193.

(54) Muraoka, T.; Adachi, K.; Ui, M.; Kawasaki, S.; Sadhukhan, N.; Obara, H.; Tochio, H.; Shirakawa, M.; Kinbara, K. A Structured Monodisperse PEG for the Effective Suppression of Protein Aggregation. *Angew. Chemie - Int. Ed.***2013**, *52* (9), 2430–2434.

(55) Whitmore, L.; Wallace, B. A. DICHROWEB, an Online Server for Protein Secondary Structure Analyses from Circular Dichroism Spectroscopic Data. *Nucleic Acids Res.***2004**, *32* (WEB SERVER ISS.), 668–673.

(56) Sreerama, N.; Woody, R. W. Estimation of Protein Secondary Structure from Circular Dichroism Spectra: Comparison of CONTIN, SELCON, and CDSSTR Methods with an Expanded Reference Set. *Anal. Biochem.***2000**, *287* (2), 252–260.

Chapter 3

Self-assembled micelles prepared from cholesterol-modified thermo-responsive polymers

3.1 Introduction

Over the past few decades, cancer has been the leading cause of deaths around the world.[1] Meanwhile, with the growing interest in the field of drug research, numerous anticancer drugs have been discovered by researchers. However, the use of these drugs, such as paclitaxel, camptothecin and so on.[2–5], into clinical use has been limited by their poor water solubility. In general, the drugs with polycyclic structure lead to poor aqueous solubility, which limits their applications.

To overcome this, the development of self- assembled polymeric micelle as a hydrophobic drug delivery system has garnered widespread attention.[6–8] Amphiphilic polymers can form micelles in aqueous solution. The hydrophobic core can load the hydrophobic drugs by hydrophobic interaction, which enhances the solubility of the hydrophobic drug and the presence of the hydrophilic shell can increase the stability of the micelles. The stronger hydrophobic effect is more beneficial for the encapsulation of hydrophobic drugs, resulting in slow release, thus increasing the circulation time. Therefore, polycyclic and hydrophobic segments can enhance the property of the micelles to load hydrophobic drugs. Meanwhile, micelles with smaller size reduces renal clearance and exhibits enhanced permeability and retention effects (EPR) at solid tumor sites for passive targeting.[9,10]

Cholesterol is a polycyclic small molecule, an essential component of mammalian cells, and is responsible for membrane fluidity and permeability, intracellular transport, signal transduction, and cell trafficking.[11–15] Since cholesterol is associated with so many membrane-related bioprocesses, so incorporation of cholesterol may be helpful for the micelles to cross the cellular membrane more easily.[16,17] Moreover, according to the empirical rule of “like dissolves like”, specifically the similarity of structure between the drugs and the hydrophobic segment in micelles enhances the encapsulation of the polycyclic drug.[18] Meanwhile, the degradability of the cholesterol also suppress the damage caused by the micelles.[17]

From the previous research regarding the tumor microenvironment, we found that the temperature and pH of the tumor cells are different from the normal tissues. [19–25]Owing to the faster metabolism, the temperature around the tumor increases to 42°C and the content of CO_2 becomes higher, resulting in the pH value around tumor tissue to be around pH 5.3. Therefore, the micelles formed by temperature responsive segment or pH-responsive segment is expected to enhance the ability of targeted release of the delivery system.[26,27]

In Chapter 2, we successfully synthesized graft copolymers which exhibits dual-thermo-responsive and pH responsive properties. In order to develop these copolymers into the hydrophobic drug delivery micelles, we have introduced cholesterol as a hydrophobic part. After being modified with cholesterol, these polymers formed micelles by self-assembly in aqueous solution. Further, hydrophobic drugs can be loaded in the core of the micelle and released by changing the temperature.

3.2 Materials and Methods

3.2.1 Materials

Sulfobetaine monomer was donated by Osaka Organic Chemical Ind., Ltd. (Osaka, Japan) and used without further purification. A 25% (w/w) ε-poly-L-lysine (PLL) (molecular weight 4000) aqueous solution was purchased from JNC Corp. (Tokyo,

Japan). Succinic anhydride (SA), 1-ethyl-3-(3-dimethylaminopropyl) carbodiimide hydrochloride (EDC-HCl) and N-Hydroxysuccinimide (NHS) were purchased from Wako Pure Chemical Ind., Ltd. (Osaka, Japan). 2-(dodecylthiocarbonothioylthio)-2-methylpropinic acid (RAFT agent), 4,4'-azobis-(4-cyanovaleric acid) (V-501, initiator), and cholesterol chloroformed were purchased from Sigma-Aldrich (St. Louis, MO).

3.2.2 Synthesis of carboxylated poly-l-lysine (PLL-SA)

PLL-SA with two different substitutions was synthesized. PLL-SA in which 50 mol% and 65 mol% of the amino groups were converted into COOH by the addition of SA were denoted as PLLSA50 (neutral at pH 7) and PLLSA65 (negative at pH 7), respectively. Briefly, PLLSA50 was synthesized by adding succinic anhydride (9.76 mmol) to the 25% (w/w) ε-poly-l-lysine (PLL) aqueous solution (10 ml), followed by stirring at 50 °C for 1 h. Similarly, PLLSA65 was synthesized by dissolving succinic anhydride (12.67 mmol) in the 25% (w/w) ε-poly-l-lysine (PLL) aqueous solution (10 ml) followed by stirring at 50 °C for 1 h. After the reaction, the products were dried in an oven overnight and vacuum-dried for 1 day.

3.2.3 Synthesis of Macro-CTA (PLLSA-RAFT agent)

We prepared two types of macro-CTA (PLLSA-RAFT agent): PLLSA50-RAFT agent and PLLSA65-RAFT agent. EDC (0.043 mmol), NHS (0.043 mmol), 2-(dodecylthiocarbonothioylthio)-2-methylpropionic acid (0.011 mmol) and 5 mL DMSO were added to a vial and stirred at 80 °C for 2 h. In another vial, 0.33 mmol PLLSA50 or PLLSA65 was dissolved in 10 mL DMSO at 130 °C. After 2 h, the two solutions were mixed together and reacted at 130 °C for 24 h. The polymer was purified by dialysis against water for 3 d using a dialysis membrane (MWCO 3.5 KDa, Repligen Corp. Waltham, MA, US). After dialysis, the polymer was obtained by lyophilization.

3.2.4 Synthesis of cho modified Macro-CTA (PLLSA-cho-RAFT agent)

0.33 mmol PLLSA50 or PLLSA65 was dissolved in 10 mL DMSO at 130 °C. After completely dissolution, 1mL DCM which contained 0.02mmol cholesterol chloroformate (cho) solution was dropped into the DMSO solution. After 6h, the solution was transferred into a dialysis membrane (MWCO 3.5 KDa, Repligen Corp. Waltham, MA, US) and dialyses against water for 3 d. After dialysis, the polymer was washed by DCM and dried in an oven.

3.2.5 Synthesis of a copolymer of PLLSA and SPB (PLLSA-cho-PSPB)

The copolymers were synthesized using the following mixture ratio: [SPB monomer]:[V-501]:[macro-CTA] = 1000:1:5. PLLSA50-cho-PSPB and PLLSA65-cho-PSPB were synthesized by dissolving the SPB monomer (6.6 mmol), V-501 (6.6 μmol) in water (45 mL), and Macro-cho-CTA (PLLSA50-cho-RAFT and PLLSA65-cho-RAFT agents, respectively) (33 μmol) was dissolved in DMSO at 90 °C. Then, the DMSO solution was added into the water solution and purged with nitrogen gas for 1 h and then stirred at 90 °C for 24 h. The polymer was then purified by dialysis against water for 3 d using a dialysis membrane (MWCO 14 KDa). After dialysis, the polymer was obtained by lyophilization.

3.2.6 Polymer characterization

The structural analyses of all polymer structures and different temperature NMR were conducted on a 400 MHz Bruker Avance III spectrometer. The data was analyzed by NMR using the Topspin 3.5 software. The number of repeating units of the graft copolymers was estimated by ^{1}H NMR from the relative area of the two peaks at around 4 ppm (corresponding to the α-protons of the substituted and unsubstituted PLL

repeating units) and that of the poly-SPB peak at around 2.2 ppm. The numbers of NH_2 groups were determined by a 2,4,6-trinitrobenzene sulfonic acid (TNBS) assay.[46] In the TNBS assay, glycine was used as the standard solution. A solution containing 0.3 ml of 250 μg/mL of solution, 1 mL 0.1% (w/v) of TNBS solution, and 2 ml of a solution containing 4% (w/v) $NaHCO_3$ and 10% (w/v) sodium dodecylsulfate was prepared. The solution was then incubated at 37 °C for 2 h. After the incubation, the absorbance of the sample solutions was measured at 335 nm using UV-vis spectroscopy (UV-1800, Shimadzu Corp., Kyoto, Japan).

3.2.7 Determination of critical micelles concentration (CMC)

The CMC of the self-assembled micelles was estimated by pyrene method. 4 μL of pyrene (1.0mM in acetone) was loaded in 10 mL test tube and completely dried under the nitrogen gas. Varied concentrations of micelles solution (0.01, 0.02, 0.05, 0.1, 0.2, 0.5, 1, 2 and 5mg/mL in PBS) were added into each tube (4 mL). Then, the solution was sonicated 30 min followed by incubation at 60 °C for 3h. After 3h the sample was cooling overnight. The fluorescence of the solubilized pyrene was measured by JASCO FP-8500 at room temperature from 350 nm to 450 nm. The excitation wavelength was 339 nm and emission wavelength 394 nm. The intensity ratio of the 394 nm and 373 nm was plotted against the concentration of micelles in order to get the CMC.

3.2.8 Partial size and zeta potential

The diameters and zeta potential of the micelle were determined by dynamic light scattering (DLS). A Zeta sizer 300 system (Malvern Instruments, Worcestershire, UK) was used to determine the hydrodynamic diameters and zeta potentials of the PLLSA50-cho-PSPB and PLLSA65-cho-PSPB. The scattering angle was 173°.

3.2.9 Atomic force Microscopy (AFM)

The AMF image was obtained by AFM5000II SPA-400 (HITACHI) using a Si probe (SI-DF20, Seiko).The sample solution (0.1% w/w) were dropped onto a fresh mica surface and air dried.

3.2.10 Transmission electron microscopy (TEM)

The morphology of the polymeric micelles was observed using a TEM H-7650 instrument (Hitachi, Tokyo, Japan). The sample was first dissolved in distilled water (5%) and after 1h sonication, the solution was diluted 500 times. 5 μL of this solution was placed on a copper grid (NS-C15 Cu150P; Stem, Tokyo, Japan). After drying at 45°C, the grid was negatively stained with 1% phosphotungstic acid (Sigma Aldrich, Steinheim, Germany) for 30 s, washed with one drop of distilled water, and air-dried.

3.2.11 Ultraviolet–visible (UV-Vis) spectroscopy for the determination of thermo- responsive properties

The turbidity of the graft copolymers was determined by UV-visible spectroscopy (UV-1800, Shimadzu Corp., Kyoto, Japan) at 550 nm. Each transmittance value was obtained at a different temperature, and there was a 12 min stabilization period at every temperature.

3.2.12 Small-angle X-ray scattering

SAXS measurements were carried out at the BL08B2, SPring-8 (Harima, Japan) using an incident X-ray with a wavelength of $\lambda = 0.124$ nm and distance from sample to detector of 16000 mm.

The2-dimensional SAXS data detected by Pilaus3-S-1M detector (172μm square pixel size) were converted into the one-dimensional intensity I(q) as a function of the scattering vector q ($q = 4\pi \sin\theta/\lambda$, where 2θ is the scattering angle, beam width 0.2×0.3mm) by circularly averaging. The covered q range was 0.008−0.2 nm^{-1}.

PLLSA50-cho-PSPB was dissolved in DDW at 5w/w % and 10μL of the solution was put in the silicone mold (and covered with kapton film and loaded onto the sample chamber. Sample was measured in the temperature region of 5−80 °C with 5 ºC /min

heating speed by attached temperature controlling plate (Linkam).

The correlation length () of the density fluctuation derived by liquid-liquid phase separation can be estimated by Ornstein-Zenike equation as follows;

$$I(q) = I(0)/(1+q^2 \quad (1)$$

The SAXS data also can be analyzed by the Guinier approximation, which can estimate the radius of gyration (Rg) by using following formula;

$$I(q) = A \exp[(-q^2Rg^2)/3] \quad (2)$$

where, A represents pre-exponential factor.

The scattering intensity corresponding to density fluctuation is seen in the region of q > 0.1 nm^{-1}. On the other hand, the scattering from aggregation described by Guinier row is observed in the lower q region (q < 0.03 nm^{-1}).[28-31]

3.2.13 Cytotoxicity Study

L929 (American Type Culture Collection, Manassas, VA, USA) cells were cultured in Dulbecco's modified Eagle's medium (DMEM, Sigma-Aldrich, St. Louis, MO), supplemented with 10% heat-inactivated fetal bovine serum in a humidified atmosphere of 5% CO_2 at 37 °C. The cytotoxicity assay was performed according to the MTT method in a 96-well plate. Briefly, 1×10^3 cells in 0.1 mL of culture media were seeded

in a 96-well plate. After incubation for 72 h, 0.1 mL of the culture medium, which contained different concentrations of the polymer, was added to the 96-well plate. After re-incubation for 24 h, 0.1 mL MTT (3-(4,5-dimethylthiazole-2-yl)-2,5-diphenyltetrazolium bromide) solution (300 μg/mL) was added to each well, and the cells were incubated for an additional 3 h. After discarding the media, 0.1 mL of DMSO was added to dissolve the purple formazan crystals that had formed. The absorbance values at 540 nm were determined using a microplate reader (versa max, Molecular Devices Co., CA, USA). The value of the absorbance indicated the number of viable cells.

3.3 Results and Discussion

3.3.1 Synthesis and polymer characterization

Synthesis of PLLSA-cho-PSPB is shown in **Scheme 3.1**. In this reaction RAFT polymerization was used. In this study, PLLSA50-cho-PSPB and PLLSA65-cho-PSPB with different degrees of substitution of SA in PLL were obtained. ^{1}H NMR and ^{13}C NMR spectroscopy were employed to characterize all the polymers. The degree of substitution (DS) of SA into PLL were determined by ^{1}H NMR and the number of RAFT agents substituted per chain and the number of cho substituted per chain

weredetermined by TNBS assay. The obtained degree of substitution of SA was almost the same in the feeding condition (**Table 3.1**). Calculations based on the results of the TNBS assay clearly reveal that approximately 1 RAFT agent was substituted on the PLLSA chain (**Table 3.1**). Meanwhile, TNBS result shows 3.6 and 2.1cho reacted with PLLSA50 chain and PLLSA65 chain.M1 and M2 represent the polymers PLLSA(50)-cho-PSPB(200) and PLLSA(65)-cho-PSPB(200), respectively. Here, 200 in the parenthesis after PSPB indicates the number of repeating units of SPB. Figure 3.1 shows the 2D NMR of the Macro-CTA-cho. The addition of cho lead to a decrease in the solubility of macro chain transfer agent in water, thus this NMR spectrum was performed in DMSO-d_6.From this spectrum we can clearly see a sample peak appeared at δ_H= 5.2 ppm δ_C= 125 ppm, this peak indicated the double bond in cholesterol. Figures 3.2–3.5 show the ^{1}H- and ^{13}C-NMR charts for M1 and M2.

Table 3.1 *Characteristics of the PLLSA-cho-PSPB.*

Entry	Polymeric micelles	Degree of substitution of SA into PLL		[b]Number of RAFT agents Substituted per chain	[c]Number of cho Substituted per chain	Number of repeating units		$M_W \times 10^{-3}$ [b]	[d]Size of the micelles	Zeta potential
		In feed	[a]In polymer			PLLSA	PSPB			
M1	PLLSA50-cho-PSPB	50%	47.0 %	1.2	3.6	31.25	172.8	54.5	105.7 ± 5.05 nm	3.53 ± 0.142
M2	PLLSA65-cho-PSPB	65%	63.6 %	0.9	1.9	31.25	132.8	43.8	50.45 ± 14.95 nm	-14.9 ± 0.872

Note: [a]Determined by ^{1}H NMR. [b]Determined by subtracting number of NH_2 in PLLSA from RAFT agent substituted PLLSA. [c]Calculated by TNBS assay. [d]Determined by DLS.

In order to evaluate of the structural changes during the phase transition, the temperature-dependent^{1}H NMR was performed. The ^{1}H NMR spectra of M1 in D_2O at different temperatures are shown in Figure 3.6.With the increase in temperature, the characteristic signals characteristic for the PLLSA block with chemical shifts at 3.9 ppm and 4.1 ppm lose most of their intensity. This indicates that with increase in temperature leads to the dehydration and aggregation of the PLLSA block. In contrast, the intensity of the peak at 3.25 ppm, which is characteristic for the PSPB block, becomes more visible. This is due to the extending of the PSPB block (owing to its transformation to a coil structure). At lower temperature, the peak at 3.25 ppm not visible likely because the shrink of PSPB block (form globule structure).This result suggests that, at lower temperature, the polymeric micelles are formed with hydrophobic PSPB as a core and hydrophilic PLLSA as a shell. the other hand, as the temperature is increased, the micelles are formed with hydrophobic PLLSA as a core and hydrophilic PSPB as a shell.

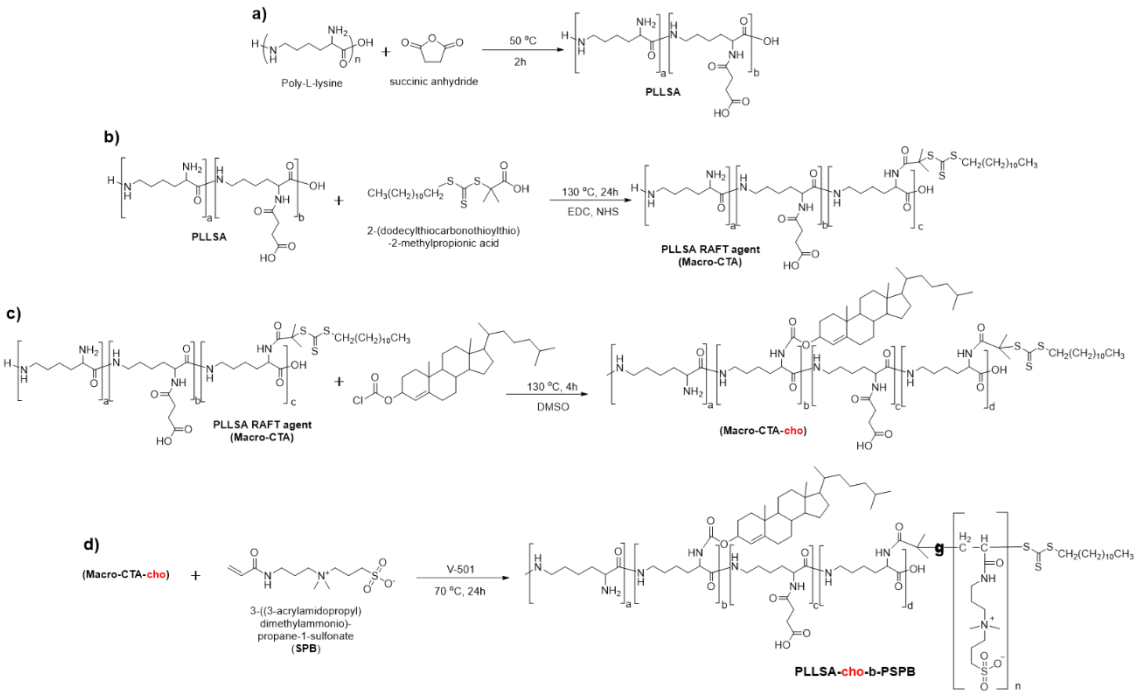

Scheme 3.1 *Schematic illustration of the synthesis of PLLSA-cho-PSPB.*

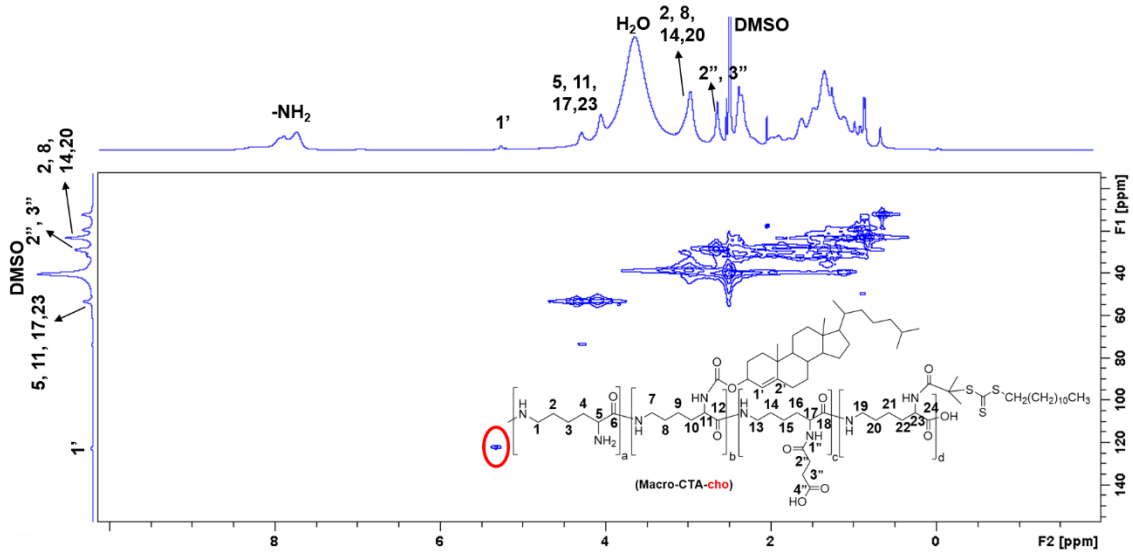

Figure 3.1 *2D NMR spectra of Macro-CTA-cho in DMSO-d6.*

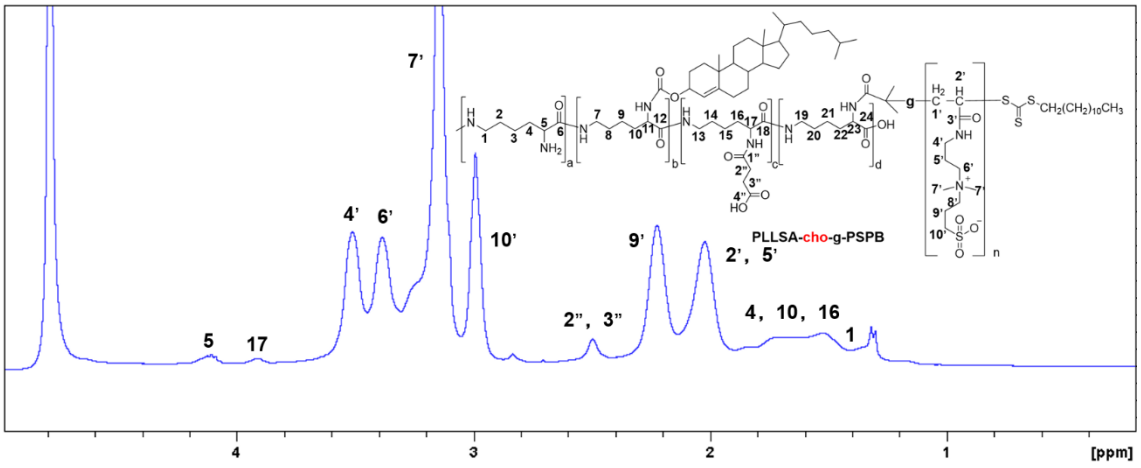

Figure 3.2 *^{1}H NMR spectra of M1 in D_2O.*

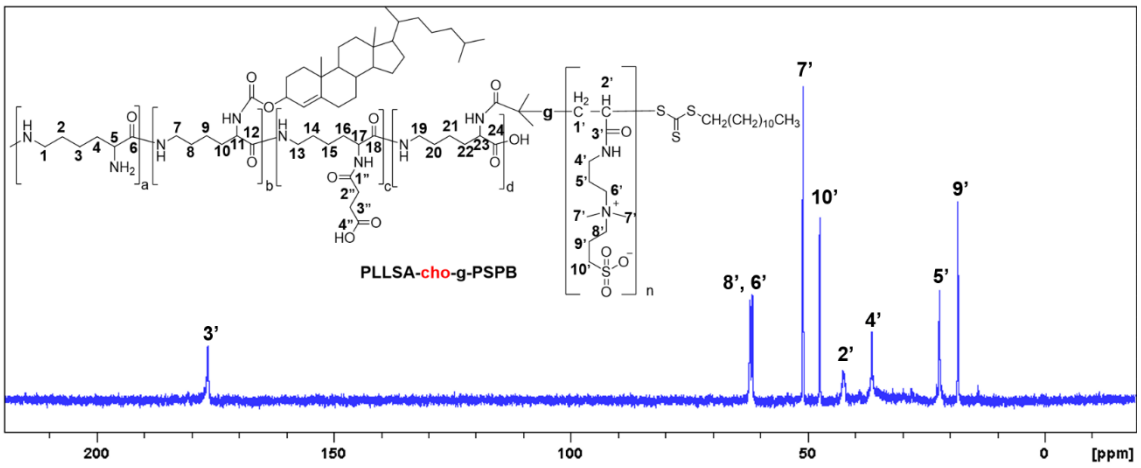

Figure 3.3 *^{13}C NMR spectra of M1 in D_2O.*

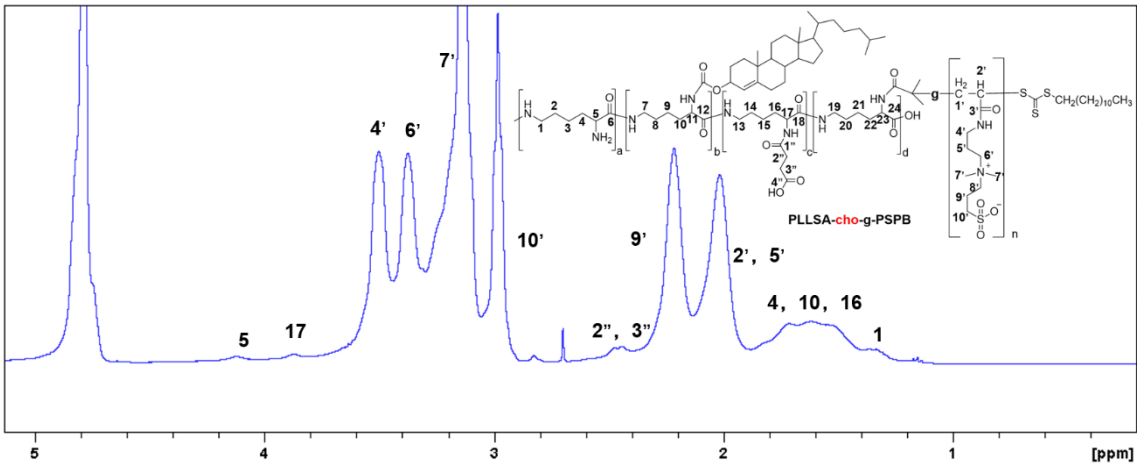

Figure 3.4 *^{1}H NMR spectra of M2 in D_2O.*

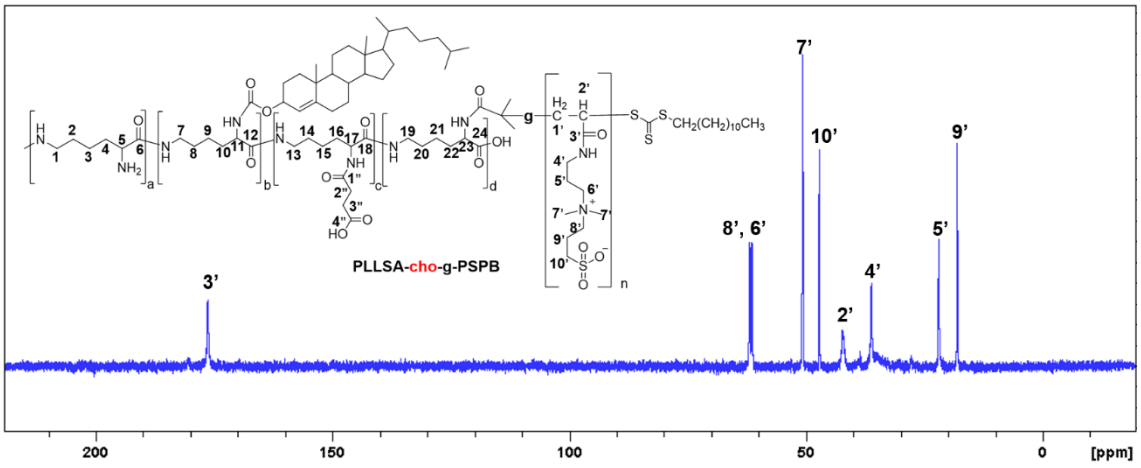

Figure 3.5 *^{13}C NMR spectra of M2 in D_2O.*

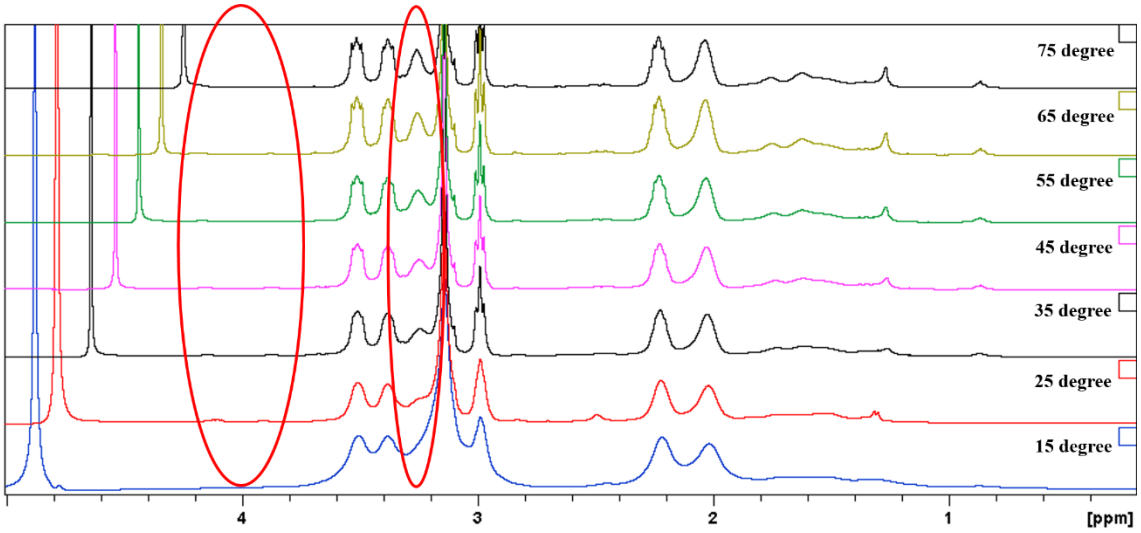

Figure 3.6 *^{1}H NMR spectra of M1 in D_2O recorded at 15-75 °C.*

3.3.2 CMC

The micelle formation by the self-assembly of PLLSA-cho-PSPB was determined by pyrene mothed. Pyrene is highly hydrophobic and preferentially migrates into the core of the micelle in the aqueous solution. The fluorescence spectra of pyrene with different

concentrations of M1 or M2 are shown in Figure 3.7. The increase of the emission intensity indicated the transformation of polymer structure change into a micelle-like structure. The CMC was estimated by the intensity ratio of the peaks at 394 nm and 373 nm. The CMC of M1 and M2 were estimated to be about 6 μg/mL.

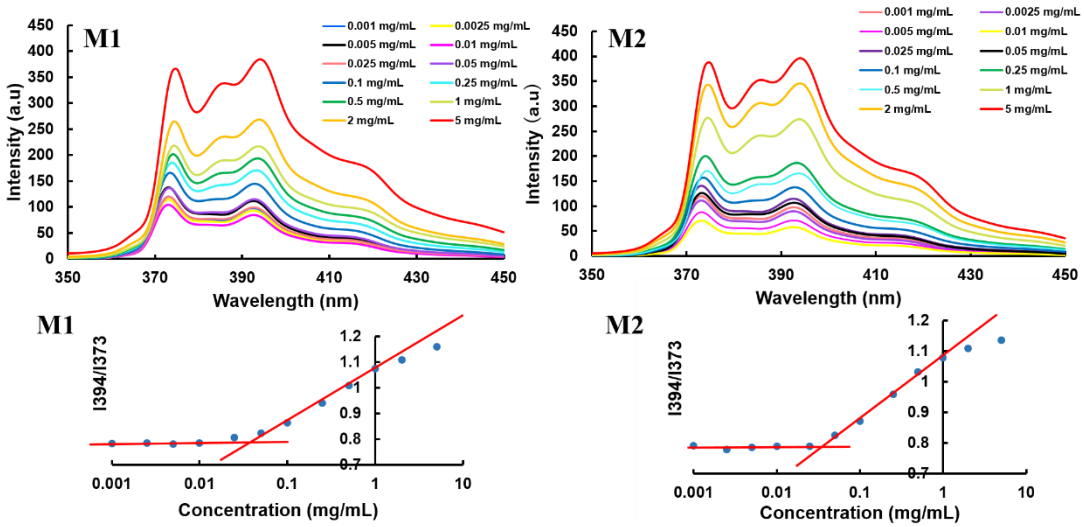

Figure 3.7 *Critical micelle concentration of M1 and M2.*

3.3.3 Partial size and zeta potential

The size of micelle is one of the important factors that can affect the drug loading, drug release and bioavailability of the micelle. The size of M1 and M2 is shown in **Table 3.1**.The size of M1 is105.7± 5.05 nm and the size of M2 is 50.45 ± 14.95 nm. The difference between the size of M1 and that of M2 is because the amount of the cho introduced. Increasein the amount of cho will increase the hydrophobic interaction

between the polymer chains. Moreover, the negative charge of the M2 may also cause the size of M2 to be smaller than that of M1.

3.3.4 The morphology of the micelles

The morphology of the micelles was visualized by TEM and AFM. **Figure 3.8** shows the TEM images of M1 and M2. The concentration of the sample was 0.1 % (w/w) in water. As seen in **Figure 3.8**, spherical micelles were obtained. The size of M1 is around 103.9 nm and the size of M2 is around 36.5 nm

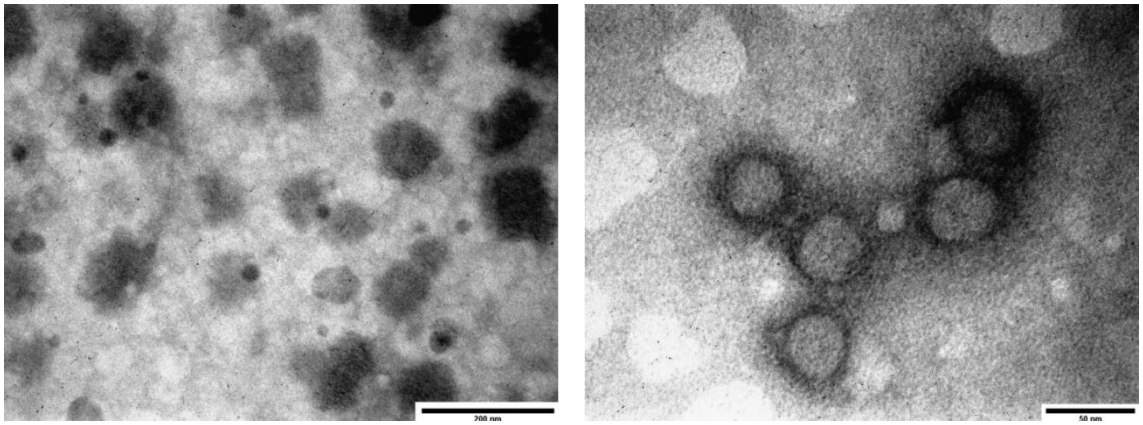

Figure 3.8 *TEM image of M1 and M2 at 0.1% (w/w).*

Figure 3.9 shows the AFM images of M1 and M2. The concentration of the sample was 0.1% (w/w) in water. Interestingly, the size of each micelle is not uniform. This is likely because of the Vander Waal interaction existing between the micelle's structures. From AFM images we can find the size of M1 also larger than that of M2. All the TEM

results and AFM results are corresponding to the DLS result. The size of micelles measured by DLS is larger than the size which, measured by TEM and AFM is due to the extension of polymer chains in

solution.

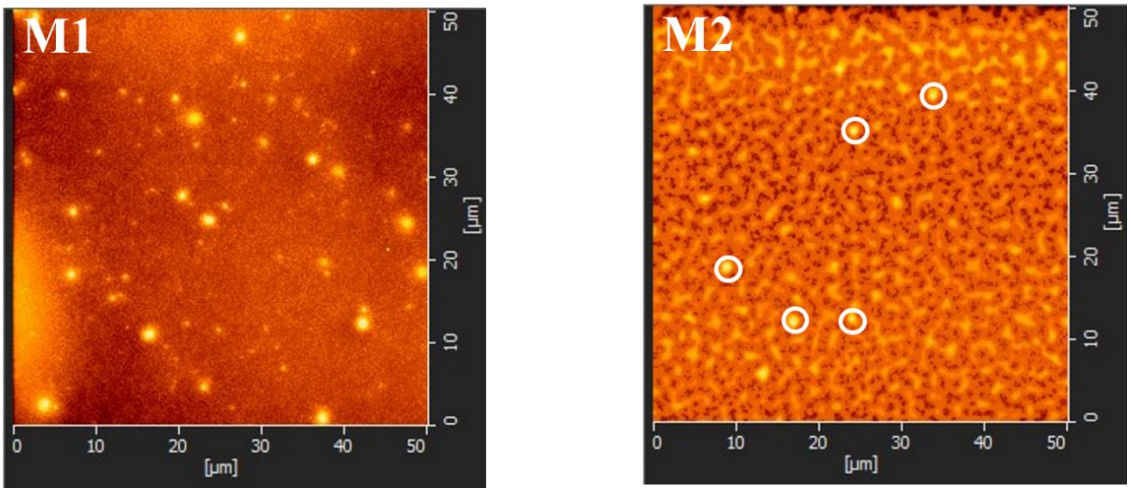

Figure 3.9 *AFM image of M1 and M2 at 0.5% (w/w).*

3.3.5 Thermoresponsive Property

The thermoresponsive property of the polymeric micelles was determined by turbidimetry in water by UV-vis spectroscopy at a 550 nm wavelength. Figure 3.10 shows the phase transition behavior of M1 and M2 at 1% (w/w) concentration. Each of the micelles display both LCST- and UCST-type phase separation behavior. With an increase in temperature, the polymer solution undergoes insoluble-soluble-insoluble transition. Upon heating, the transmittance of the solution increases and as the

temperature is further increased, the transmittance of the solution starts decreasing. At low temperatures, the graft copolymer (SPB segment) exhibits UCST-type transition, and at high temperatures, the graft copolymer (PLLSA segment) exhibits LCST-type transition. For M1 (**Figure 3.10a**), at 10 °C, the polymer solution is turbid, and the transmittance increases with the temperature. When the temperature reaches 20 °C, the transmittance reaches its maximum value. However, as the temperature increases beyond 24 °C, the transmittance starts decreasing. From around 26 °C to 70 °C, the polymer exhibits LCST behavior (PLLSA segment). The transmittance decreases with further increases in temperature because of the gradual dehydration of the PLLSA chain (LCST transition). Similarly, in the case of M2 (**Figure 3.10b**), the transmittance of the solution increases when the temperature increases from 10 °C to 30 °C. This is followed by a decrease in transmittance with further increases in the temperature, up to 70 °C. Figure 3.10 clearly shows that the polymer exhibits both a UCST and a LCST behavior. In addition, we observe that the maximum transmittance value of the M1 and M2was smaller than that of the liner polymer (P1 and P2); this is because of introduce cholesterol into M1 and M2. The addition of hydrophobic cholesterol decreases the transmittance of the micelle. Meanwhile the temperature of phase transaction are decrease by compare with the liner polymer at the same concertation.

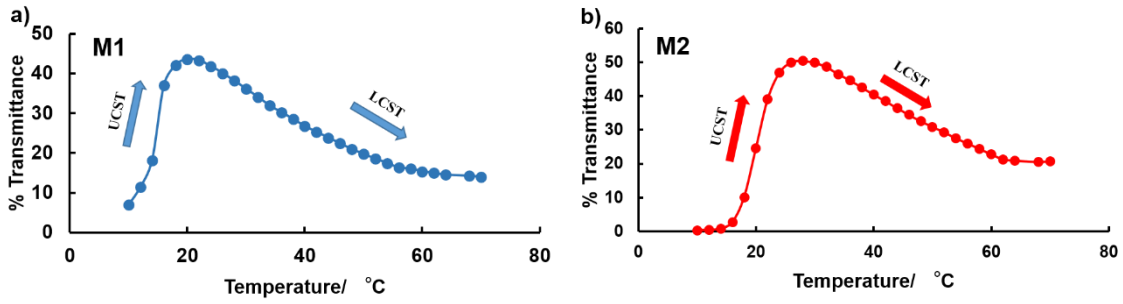

Figure 3.10 *Relative transmittance of polymer solutions of (a) M1 and (b) M2 at 1% (w/w) concentration in water.*

3.3.6 Small-angle X-ray scattering

Figure 3.11shows the SAXS curves obtained of M1 in water during heating. On increase the temperature, the intensity of q at small q value was decreasing. It represents USCT type phase separation and the separation size can be calculated with Guinier approximation and the size (R_g) was calculated to be around 260 to 200 nm (Figure 3.12a) and c)).This can be explained by a large aggregation that was diminished by the coil globule transition of PSPB part. And high q value area also shows the intensity change by temperature. In this region, the intensity of the q value increased on increasing the temperature. This is due to LCST type phase separation of PLL part. Here, I evaluated Ornstein Zernike approximation and calculated the correlation length (Figure 3.12b) and d)). This value is smaller than R_g, but molecular level fluctuation occurred in LCST. Also, visible LCST temperature was observed much earlier by SAXS,

compared to UV-vis, hence it can be argued that SAXS detected the earlier region of separation. In a microscopic view, phase transition begins around 30 degrees.

Interestingly, SAXS results revealed that UCST and LCST phenomenon occurred at entirely different scale, in terms of size. For UCST in PSPB, a large change in particle size was observed at around Rg=200. This is likely due to coil-globule transition in PSPB. This is well supported by the observation of spherical structures in TEM and AFM. Decrease in intensity of SAXS at low q region on heating (due to UCST) indicates that electron density in particles decreases as a result of globule to coil transition. Further, decrease in size clearly suggests that some of polymer chains could be dissolved into solvent. In contrast, LCST in PLLSA was observed with a much smaller change in the size of correlation length between the two phases with higher and lower density. This might be due to the liquid-liquid phase transition of PLLSA.

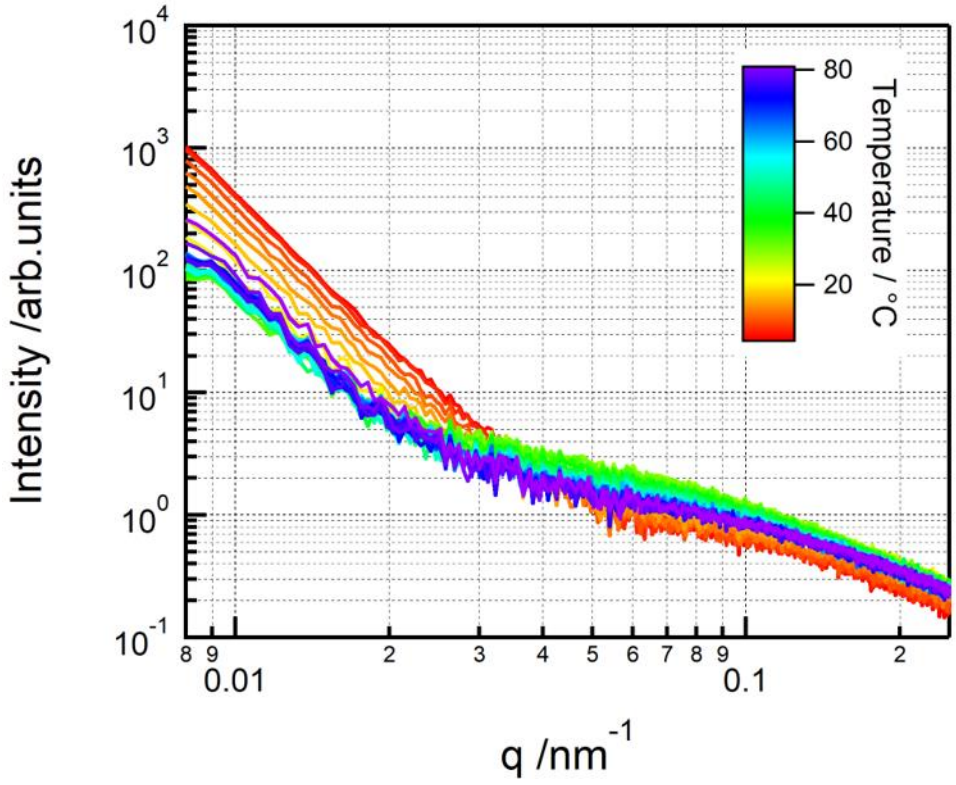

Figure 3.11 *SAXS curves of 5% w/w M1 at various temperature in aqueous solution.*

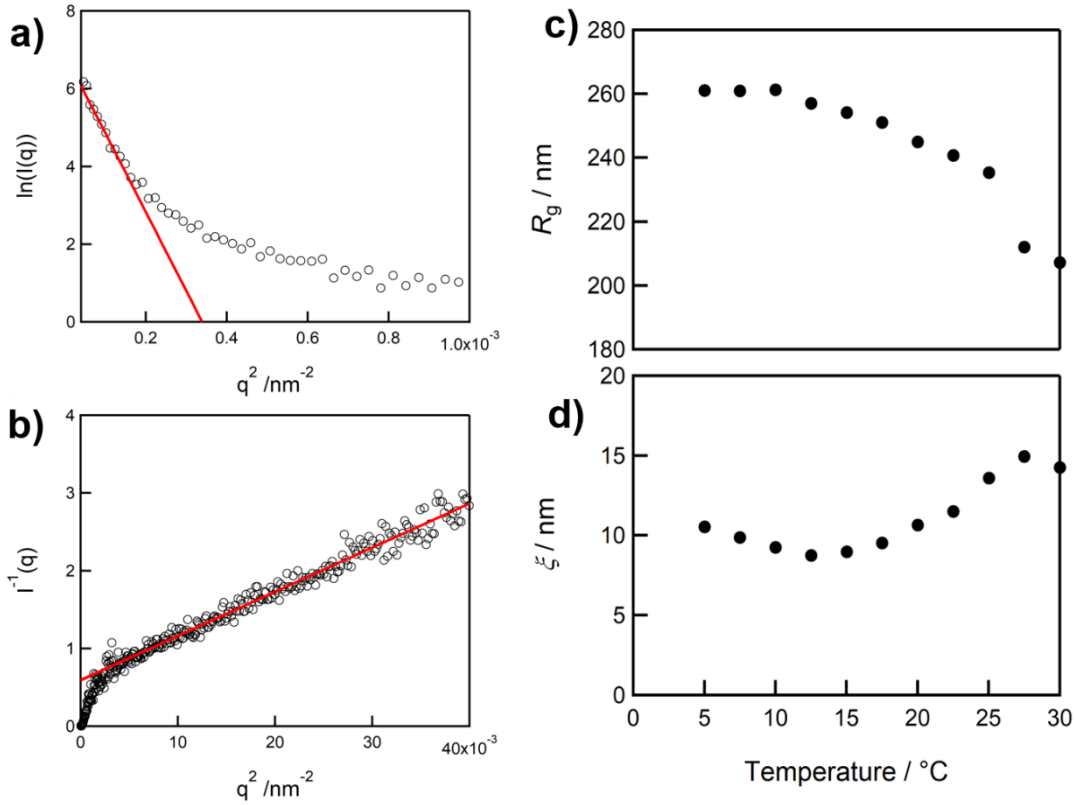

Figure 3.12 *a) Guinier plot analysis at low q region. b) Ornsyein-Zernike plot analysis at high q region. c) temperature responsive radius of gyration estimated by Guinier plot and d) correlation length estimated by Ornsyein-Zernike plot.*

3.3.7 Cytotoxicity Assay

Figure 3.13shows the cytotoxicity of the micelles, and the results clearly demonstrate that both M1 and M2 show very low toxicity, at 1% concentrations, the cell viability was above 80%. Cytotoxicity was evaluated by IC_{50}(half maximal inhibitory concentration), which is, the concentration of the test compound needed to kill half of the cells, IC_{50} was not observed at these concentrations. Low toxicity indicates that these micelles are extremely biocompatible and can be safely used in living organisms.

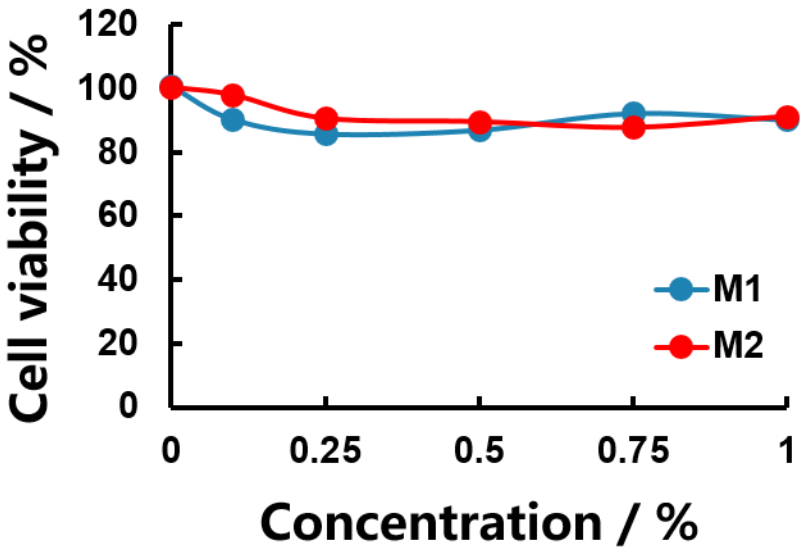

Figure 3.13 *Cytotoxicity of the micelles. L929 cells were treated with different concentrations of polymers: M1 (blue closed circles) andM2 (red closed circles).*

3.4 Conclusion

In conclusion, I synthesized and performed molecular characterization of two dual-thermo-responsive polymers, PLLSA50-cho-PSPB and PLLSA65-cho-PSPB. Both the polymers are able to form spherical stable micellar structures with diameters of ca. 157 and ca. 208 nm, respectively, in aqueous solution. The CMC values of both copolymers were found to be very low due to the addition of hydrophobic cholesterol. Presence of large amount of hydrophobic cholesterol content is expected to increase the solubilization capacity for the water-insoluble drug. The low cytotoxicity of the micelles will reduce systemic toxicity, thus making these micelles a very good candidates for the delivery system for hydrophobic drugs.

3.5 References

(1) Ercole, F.; Whittaker, M. R.; Quinn, J. F.; Davis, T. P. Cholesterol Modified Self Assemblies and Their Application to Nanomedicine. *Biomacromolecules***2015**, *16* (7), 1886–1914.

(2) Laskar, P.; Samanta, S.; Ghosh, S. K.; Dey, J. In Vitro Evaluation of PH-Sensitive

Cholesterol-Containing Stable Polymeric Micelles for Delivery of Camptothecin. *J. Colloid Interface Sci.***2014**, *430*, 305–314.

(3) Yokoyama, M.; Fukushima, S.; Uehara, R.; Okamoto, K.; Kataoka, K.; Sakurai, Y.; Okano, T. Characterization of Physical Entrapment and Chemical Conjugation of Adriamycin in Polymeric Micelles and Their Design for in Vivo Delivery to a Solid Tumor. *J. Control. Release***1998**, *50* (1–3), 79–92.

(4) Kim, T. Y.; Kim, D. W.; Chung, J. Y.; Shin, S. G.; Kim, S. C.; Heo, D. S.; Kim, N. K.; Bang, Y. J. Phase I and Pharmacokinetic Study of Genexol-PM, a Cremophor-Free, Polymeric Micelle-Formulated Paclitaxel, in Patients with Advanced Malignancies. *Clin. Cancer Res.***2004**, *10* (11), 3708–3716.

(5) Lee, A. L. Z.; Venkataraman, S.; Sirat, S. B. M.; Gao, S.; Hedrick, J. L.; Yang, Y. The Use of Cholesterol-Containing Biodegradable Block Copolymers to Exploit Hydrophobic Interactions for the Delivery of Anticancer Drugs. *Biomaterials***2012**, *33* (6), 1921–1928.

(6) Lu, C.; Jiang, L.; Xu, W.; Yu, F.; Xia, W.; Pan, M.; Zhou, W.; Pan, X.; Wu, C.; Liu, D. Poly(Ethylene Glycol) Crosslinked Multi-Armed Poly(ε-Benzyloxycarbonyl-L-Lysine)s as Super-Amphiphiles: Synthesis, Self-Assembly, and Evaluation as Efficient Delivery Systems for Poorly Water-Soluble

Drugs. *Colloids Surfaces B Biointerfaces***2019**, *182* (July), 110384.

(7) Jelonek, K.; Li, S.; Wu, X.; Kasperczyk, J.; Marcinkowski, A. Self-Assembled Filomicelles Prepared from Polylactide/Poly(Ethylene Glycol) Block Copolymers for Anticancer Drug Delivery. *Int. J. Pharm.***2015**, *485* (1–2), 357–364.

(8) Rajagopal, K.; Mahmud, A.; Christian, D. A.; Pajerowski, J. D.; Brown, A. E. X.; Loverde, S. M.; Discher, D. E. Curvature-Coupled Hydration of Semicrystalline Polymer Amphiphiles Yields Flexible Worm Micelles but Favors Rigid Vesicles: Polycaprolactone-Based Block Copolymers. *Macromolecules***2010**, *43* (23), 9736–9746.

(9) Kalyane, D.; Raval, N.; Maheshwari, R.; Tambe, V.; Kalia, K.; Tekade, R. K. Employment of Enhanced Permeability and Retention Effect (EPR): Nanoparticle-Based Precision Tools for Targeting of Therapeutic and Diagnostic Agent in Cancer. *Mater. Sci. Eng. C***2019**, *98* (January), 1252–1276.

(10) Greish, K.; Fang, J.; Inutsuka, T.; Nagamitsu, A.; Maeda, H. Macromolecular Therapeutics Tumour Targeting. *Clin. Pharmacokinet.***2003**, *42* (13), 1089–1105.

(11) Yeagle, P. L. Modulation of Membrane Function by Cholesterol. *Biochimie***1991**, *73* (10), 1303–1310.

(12) Yeagle, P. L. Cholesterol and the Cell Membrane. *BBA - Rev. Biomembr.***1985**,

822 (3–4), 267–287.

(13) Incardona, J. P.; Eaton, S. Cholesterol in Signal Transduction. *Curr. Opin. Cell Biol.***2000**, *12* (2), 193–203.

(14) Frederick R. Maxfield & Ira Tabas. Role of Cholesterol and Lipid Organization in Disease. *Nature***2005**, *438*, 612–621.

(15) Kai Simonsl and Elina Ikonen. How Cells Handle Cholesterol. *Science (80-.).* **2000**, *290* (December), 1721–1726.

(16) Wang, Y.; Wang, H.; Liu, G.; Liu, X.; Jin, Q.; Ji, J. Self-Assembly of near-Monodisperse Redox-Sensitive Micelles from Cholesterol-Conjugated Biomimetic Copolymers. *Macromol. Biosci.***2013**, *13* (8), 1084–1091.

(17) Hosta-Rigau, L.; Zhang, Y.; Teo, B. M.; Postma, A.; Städler, B. Cholesterol - A Biological Compound as a Building Block in Bionanotechnology. *Nanoscale***2013**, *5* (1), 89–109.

(18) Zheng, S.; Xie, Y.; Li, Y.; Li, L.; Tian, N.; Zhu, W.; Yan, G.; Wu, C.; Hu, H. Development of High Drug-Loading Nanomicelles Targeting Steroids to the Brain. *Int. J. Nanomedicine***2013**, *9* (1), 55–66.

(19) Gammas, S.; Suzuki, K.; Sone, C.; Sakurai, Y.; Kataoka, K.; Okano, T. Thermo-Responsive Polymer Nanoparticles with a Core-Shell Micelle Structure as

Site-Specific Drug Carriers. *J. Control. Release***1997**, *48* (2–3), 157–164.

(20) Ganta, S.; Devalapally, H.; Shahiwala, A.; Amiji, M. A Review of Stimuli-Responsive Nanocarriers for Drug and Gene Delivery. *J. Control. Release* **2008**,*126* (3), 187–204.

(21) Rijcken, C. J. F.; Soga, O.; Hennink, W. E.; Nostrum, C. F. va. Triggered Destabilisation of Polymeric Micelles and Vesicles by Changing Polymers Polarity: An Attractive Tool for Drug Delivery. *J. Control. Release***2007**, *120* (3), 131–148.

(22) Schmaljohann, D. Thermo- and PH-Responsive Polymers in Drug Delivery. *Adv. Drug Deliv. Rev.***2006**, *58* (15), 1655–1670.

(23) De Las Heras Alarcón, C.; Pennadam, S.; Alexander, C. Stimuli Responsive Polymers for Biomedical Applications. *Chem. Soc. Rev.***2005**, *34* (3), 276–285.

(24) Chilkoti, A.; Dreher, M. R.; Meyer, D. E.; Raucher, D. Targeted Drug Delivery by Thermally Responsive Polymers. *Adv. Drug Deliv. Rev.***2002**, *54* (5), 613–630.

(25) Kim, I. S.; Jeong, Y. Il; Cho, C. S.; Kim, S. H. Thermo-Responsive Self-Assembled Polymeric Micelles for Drug Delivery in Vitro. *Int. J. Pharm.***2000**, *205* (1–2), 165–172.

(26) Hu, Y.; Darcos, V.; Monge, S.; Li, S. Thermo-Responsive Drug Release from Self-Assembled Micelles of Brush-like PLA/PEG Analogues Block Copolymers. *Int. J.*

*Pharm.***2015**, *491* (1–2), 152–161.

(27) Huang, X.; Liao, W.; Zhang, G.; Kang, S.; Zhang, C. Y. PH-Sensitive Micelles Self-Assembled from Polymer Brush (PAE-g-Cholesterol)-b-PEG-b-(PAE-g-Cholesterol) for Anticancer Drug Delivery and Controlled Release. *Int. J. Nanomedicine***2017**, *12*, 2215–2226.

(28) Kikhney, A. G.; Svergun, D. I. A Practical Guide to Small Angle X-Ray Scattering (SAXS) of Flexible and Intrinsically Disordered Proteins. *FEBS Lett.***2015**, *589* (19), 2570–2577.

(29) Peyronel, F.; Pink, D. A. Ultra-Small Angle X-Ray Scattering. *Struct. Anal. Edible Fats***2018**, *8* (1), 267–285.

(30) Akiba, I.; Terada, N.; Hashida, S.; Sakurai, K. Encapsulation of a Hydrophobic Drug into a Polymer-Micelle Core Explored with Synchrotron SAXS. **2010**, *26* (13), 7544–7551.

(31) Kageyama, A.; Yanase, M.; Yuguchi, Y. Structural Characterization of Enzymatically Synthesized Glucan Dendrimers. *Carbohydr. Polym.***2019**, *204*, 104–110.

Chapter 4

General conclusion

The research in this thesis focused on synthesizing multi stimuli-responsive polymers, which contains PLLSA block. In order to development materials with new applications of the PLLSA, I synthesized graft polymers which contains two different polyampholyte segments. And then I modified it with a hydrophobic moiety, which allowed them to form micelles in aqueous solution. Moreover, the synthesized polymers were used as suppressors of protein aggregation and have the potential to become a hydrophobic drug delivery system.

Chapter 2: I synthesized two dual-thermo- and pH-responsive graft copolymers by RAFT polymerization. These graft copolymers contain two different polyampholyte segments (PLLSA and PSPB). The presence of two zwitterionic segments allows the graft copolymer to exhibit a dual-temperature responsive property. The present study shows that these polymers can suppress protein aggregation under severe stress. A very high protein protection efficiency was observed after heating at very high temperatures, and the secondary structure of the lysozyme was also retained in the presence of these graft copolymers. The high efficiency of these polymers was because it acts as a molecular shield and decreases the collisions between proteins. Moreover, easy tunability can potentially allow these graft copolymers to be used in a variety of applications.

Chapter 3: The thermoresponsive polymeric micelles with cholesterol modified were fabricated. These micelles were formed by self-assembly in an aqueous solution. The addition of cholesterol decreased the CMC of the micelles. Meanwhile, these micelles formed stable spherical structures. Further, these polymeric micelles can be developed as a hydrophobic drug delivery system.

For future work, polymer containing PLLSA segment, should be exploredto respond to other stimuli and to develop such as thermo- and light-responsive polymers, thermos-

and redox-responsive polymers. Moreover, the degradable micelle systems should be considered. Hopefully, the polymer in which the content PLLSA segment can be used in other applications.

Achievements

Publication

Dandan Zhao, Robin Rajan and Kazuaki Matsumura. Dual Thermo- and PH-Responsive
Behavior of Double Zwitterionic Graft Copolymers for Suppression of Protein Aggregation and Protein Release. *ACS Appl. Mater. Interfaces***2019**, *11*, 39459–39469.

RelatedPublication

Sana Ahmed, Tadashi Nakaji-Hirabayashi, Robin Rajan, Dandan Zhao and Kazuaki Matsumura. Cytosolic delivery of quantum dots mediated by freezing and hydrophobic polyampholytes in RAW 264.7 cells. Journal of Materials Chemistry B 2019, DOI:10.1039/C9TB01184F

Conferences:

Dandan Zhao, Robin Rajan and Kazuaki Matsumura
27th Annual Meeting of MRS-J, Yokohama, Japan, 5-7 Dec 2017
Dual-thermoresponsive polymeric systems exhibiting UCST and LCST for biomedical applications

Dandan Zhao, Robin Rajan and Kazuaki Matsumura
Hokuriku Biomaterials conference, Nagano, Japan, 15 Dec 2017

Synthesis of dual-thermo- and pH- responsive polymer for protein delivery

Dandan Zhao, Robin Rajan and Kazuaki Matsumura
67th SPSJ Symposium on Macromolecules, Sapporo, Japan, 12-14 Sep 2018
Synthesis of multi- stimuli-responsive polymer for protein delivery

Dandan Zhao, Robin Rajan and Kazuaki Matsumura
Spring 2019 ACS National Meeting & Exposition, USA, Florida, Orlando, March 31-April 4 2019.
The synthesis and characterization of the dual-thermo-responsive diblock copolymer.

Dandan Zhao, Robin Rajan and Kazuaki Matsumura
Tissue Engineering & Regenerative MedicineInternational Society - AP Chapterand the 7th Asian Biomaterials Congress,AUS, Brisbane, October14-17 2019.
pH-responsive polymeric delivery system for protein delivery and protection.

Acknowledgement

Firstly, I would like to thank my supervisor, Prof. Kazuaki Matsumura for his support, assistance, guidance, motivation and good suggestions for solving problems throughout the completion of my doctoral study. I really appreciate all his contributions of time, opinion, and funding to make my Ph.D. experience productive and stimulating. Without his support, I could not have stayed in Japan to finish my Ph.D. study.

Second, I would like to thank my Assistant Prof. Robin Rajan. Without his help I could not successfully start my Ph.D. study and could not successfully publish my first English paper. I also deeply appreciate Prof. Tatsuo Kaneko for his support for my minor research.

I would like to thank all my fellow lab-mates for their encouragement and support. Especially thank Keiko Kawamoto san for assistance in cytotoxicity assayand HaritPitakjakpipopsan for assistance in the taking of proteinaggregation inhibition photographs.

Finally, I am really grateful to my family for their understanding and support.